https://doi.org/10.5194/egusphere-2023-3038
Preprint. Discussion started: 15 January 2024

Yakima River Basin Water Column Respiration is a Minor Component of River Ecosystem Respiration

Stephanie G. Fulton[1*], Morgan Barnes[1], Mikayla A. Borton[1,2], Xingyuan Chen[1], Yuliya Farris[1], Brieanne Forbes[1], Vanessa A. Garayburu-Caruso[1], Amy E. Goldman[1], Samantha Grieger[3], Robert O. Hall, Jr.[4], Matthew H. Kaufman[1], Xinming Lin[1], Erin McCann[1], Sophia A. McKever[1], Allison Myers-Pigg[3], Opal Otenburg[3], Aaron C. Pelly[1,5], Huiying Ren[1], Lupita Renteria[1], Timothy D. Scheibe[1], Kyongho Son[1], Jerry Tagestad[1], Joshua M. Torgeson[1], James C. Stegen[1,5*]

[1]Pacific Northwest National Laboratory, Richland, Washington USA
[2]Colorado State University, Fort Collins, CO USA
[3]Pacific Northwest National Laboratory, Marine and Coastal Research Laboratory, Sequim, Washington USA
[4]Flathead Lake Biological Station, University of Montana, Polson, Montana USA
[5]School of the Environment, Washington State University Tri-Cities, Richland, Washington USA

Correspondence to: James C. Stegen (james.stegen@pnnl.gov) and Stephanie G. Fulton (stephgfulton@gmail.com)

Abstract

Aerobic respiration of organic matter is a key metabolic process influencing carbon (C) biogeochemistry in aquatic ecosystems. Anthropogenic and environmental perturbations to stream ecosystem metabolism can have deleterious effects on downstream water quality. Various environmental features of rivers also influence stream metabolism, including physical (e.g., discharge, light, flow regimes) and chemical factors (nutrients, organic matter) and watershed characteristics (e.g., stream size or drainage area, land use). The relative proportion of surface water contact with benthic sediments has been considered the primary driver of ecosystem processes, including ecosystem respiration (ER). While aquatic ecosystem respiration occurs in the water column (ER_{wc}) and in benthic sediments—including surficial and subsurface sediments (ER_{sed})—ER_{sed} has long been assumed to be the primary contributor to whole-river ecosystem respiration (ER_{tot}). Recent studies show, however, that somewhere along the river continuum (e.g., 5^{th}–9^{th} order), rivers transition from being dominated by benthic processes to being dominated by water column processes. Yet few metabolism studies have parsed contributions from the water column (ER_{wc}) to ER_{tot}, making it difficult to evaluate the relative magnitude and importance of ER_{wc} across the river continuum and across biomes. In this study, we used the Yakima River basin, Washington, USA, to increase our understanding of basin-scale variation in ER_{wc}. We collected ER_{wc} data and water chemistry samples in triplicate at 47 sites in the Yakima River basin distributed across Strahler stream orders 2–7 and different hydrological and biophysical settings during summer baseflow conditions in 2021. We found that observed ER_{wc} rates were consistently slow throughout the basin during baseflow conditions, ranging from −0.11–0.03 mg O_2 L^{-1} d^{-1}, and were generally at the very slow end of the range of published ER_{wc} literature values. When compared to reach-scale ER_{tot} rates predicted for rivers across the conterminous United States (CONUS), the very slow ER_{wc} rates we observed throughout the Yakima River basin indicate that ER_{wc} is likely a small component of ER_{tot} in this basin. Despite these slow rates, ER_{wc} nonetheless shows spatial variation across the Yakima River basin that was well explained by watershed characteristics and water chemistry. Multiple linear regression model results show that nitrate (NO_3-N), dissolved organic carbon (DOC), and temperature together explained 41.5 % of the spatial variation in ER_{wc}. Supporting the findings of other studies, we found that ER_{wc} increased linearly with increasing NO_3-N, increasing DOC, and increasing temperature. We hypothesize that low concentrations of nutrients, DOC, and low temperatures in the water column, coupled with low TSS concentrations, likely contribute to the slow ER_{wc} rates observed throughout the Yakima River

https://doi.org/10.5194/egusphere-2023-3038
Preprint. Discussion started: 15 January 2024

basin. Because ER_{tot} measurements integrate contributions from water column respiration and sediment-associated respiration (ER_{sed}), estimating ER_{tot} in cold, clear, low nutrient rivers like those in the Yakima River basin with very slow ER_{wc} will essentially measure contributions from ER_{sed}.

1 Introduction

Aerobic respiration is a key metabolic process influencing biogeochemical cycling through the processing of organic matter (OM) in aquatic ecosystems (Reisinger et al., 2016; Hall and Hotchkiss, 2017; Genzoli and Hall, 2016; Allan et al., 2021a). Anthropogenic and environmental perturbations (e.g., land use/land cover change, fire, flooding) to stream ecosystem metabolic processes such as gross primary production (GPP) and ecosystem respiration (ER) can lower downstream water quality (Zhang and Chadwick, 2022; Diamond et al., 2021a; Alnoee et al., 2021). Climate change-related alterations in temperature and precipitation have affected the frequency, intensity, and scale of the impacts from these disturbances on streams and rivers. Environmental features of rivers also influence their metabolism, including physical factors such as discharge (Bernhardt et al., 2022; Isabel et al., 2022; Hensley et al., 2019; Hotchkiss et al., 2015), flow regimes (Bernhardt et al., 2018; Ahmed and Abdul-Aziz, 2022; Clapcott and Barmuta, 2010), flow extremes (Hensley et al., 2019; Demars, 2019; Schiller et al., 2019), light availability (Bernhardt et al., 2022; Savoy and Harvey, 2021; Kirk et al., 2021; Cory et al., 2014; Savoy et al., 2021), and temperature (Hornbach, 2021; Jankowski and Schindler, 2019; Hotchkiss and Hall, 2014; Nakano et al., 2022); chemical factors including the availability of nutrients (Mulholland et al., 2008; Hoellein et al., 2007; Reisinger et al., 2021; Reisinger et al., 2015; Hall and Tank, 2003; Mulholland et al., 2001; Carlson and Poole, 2022) and the amount and quality of OM inputs and dissolved organic C (DOC) (Allan et al., 2021b; Garayburu-Caruso et al., 2020a; Bertuzzo et al., 2022; Zarnetske et al., 2011; Ellis et al., 2012); and watershed characteristics such as stream size or drainage area (Finlay, 2011; Hotchkiss et al., 2015), hydrologic connectivity (Hotchkiss et al., 2015; Rocher-Ros et al., 2019; Demars, 2019), watershed geomorphology (Jankowski and Schindler, 2019), and land use and land cover (Bernot et al., 2010; Bertuzzo et al., 2022; Hoellein et al., 2013; Trentman et al., 2021; Gu et al., 2022).

Historically, lotic metabolism studies have been conducted in headwater streams characterized by the relatively large contact area between surface water and benthic sediments (for purposes of this paper, benthic sediments include surficial, hyporheic or subsurface, and bank sediments) (Peterson et al., 2001; Alexander et al., 2007; Mulholland et al., 2008; Gomez-Velez et al., 2015; Findlay, 1995; Battin et al., 2008). Early metabolism studies typically focused primarily on estimating reach-scale ER (referred to hereinafter as ER_{tot}) or on the contributions of benthic sediment-associated respiration (ER_{sed}) to ER_{tot} (Uzarski et al., 2004; Grimm and Fisher, 1984), with less attention on the relative contribution of water column respiration (ER_{wc}) to ER_{tot} (Son et al., 2022; Gardner and Doyle, 2018). For example, Grimm and Fisher (1984) measured respiration in both surficial sediments and the hyporheic zone in a Sonoran Desert stream and found that, on average, ER_{sed} contributions comprised 76 % of ER_{tot}. Similarly, Naegeli and Uehlinger (1997) measured respiration rates in the hyporheic zone of a gravel bed river using closed chambers and found that ER_{sed} contributions ranged from 76–96 % of ER_{tot}. However, recent advances in computer software and processing speeds, coupled with the increased availability of high temporal resolution time series sensor data (e.g., dissolved oxygen (DO), temperature, and river depth), have extended the reach of studies beyond the headwaters, enabling researchers to estimate GPP and ER for hundreds of mid-sized (i.e., non-wadeable) rivers and headwater streams across the conterminous United States (CONUS) (Bernhardt et al., 2018; Bertuzzo et al., 2022; Savoy et al., 2019; Appling et al., 2018a; Appling et al., 2018b, c) and entire stream networks (Segatto et al., 2021; Koenig et al., 2019; Savoy and Harvey, 2021; Diamond et al., 2021b; Mejia et al., 2019; Rodríguez-

https://doi.org/10.5194/egusphere-2023-3038
Preprint. Discussion started: 15 January 2024

Castillo et al., 2019). Additionally, we know that the relative contribution of the water column to reach-scale processes such as GPP, ER, and carbon (C) and nitrogen (N) cycling are greater than previously assumed (Gardner and Doyle, 2018; Battin et al., 2008; Alexander et al., 2000; Reisinger et al., 2021; Reisinger et al., 2016; Reisinger et al., 2015; Marzadri et al., 2017), an assumption attributed to the historic lack of empirical data in non-wadeable or mid-sized rivers (Reisinger et al., 2015; Liu et al., 2013; Tank et al., 2008). Some biogeochemical processes such as denitrification, a process commonly assumed to occur primarily in benthic sediments (Mulholland et al., 2008; Alexander et al., 2000; Hall and Tank, 2003), can occur in the water column of rivers and streams (Liu et al., 2013; Peterson et al., 2001; Reisinger et al., 2021; Battin et al., 2008; Marzadri et al., 2017; Reisinger et al., 2016). Examining the relative contributions of benthic sediments and the water column to reach-scale processes, Reisinger et al. (2016) estimated that water column denitrification accounted for 0–85 % of reach-scale denitrification and 39–85 % of reach-scale ER_{tot} (i.e., ER_{wc} + ER_{sed}), concluding that the water column can be more biogeochemically active than benthic sediments. Furthermore, water column processes become more important as rivers increase in size and that along the river continuum material processing transitions from being a benthic-dominated process to a water column-dominated process (Gardner and Doyle, 2018; Reisinger et al., 2015; Reisinger et al., 2016; Del Giorgio and Williams, 2005).

While water column processes can contribute significantly to ER_{tot} (Vannote et al., 1980; Reisinger et al., 2021; Roley et al., 2023), there is a paucity of direct ER_{wc} measurements. This lack of data makes it difficult to evaluate the magnitude of ER_{wc}, the contribution of ER_{wc} to ER_{tot}, or determine which factors control basin-scale variation in ER_{wc}. However, recent work has shown that across 15 mid-sized midwestern and western rivers primary production and respiration in the water column were controlled by a suite of factors: ER_{wc} was driven by physical and chemical drivers (e.g., turbidity, nutrient concentrations) while water column GPP responded more to biological factors (e.g., chlorophyl a, ash free dry mass) (Reisinger et al., 2021). In this study, we used the Yakima River basin in Washington, USA, as an environmentally diverse river network to advance our understanding of basin-scale spatial variation in ER_{wc}. We demonstrate that the Yakima River basin is representative of the larger Columbia River basin, which spans the northwest region of the CONUS. The Yakima River basin encompasses climatic regimes, biomes, physical settings, and land use conditions commonly found throughout the Columbia River basin and other basins across the western CONUS. We took advantage of the basin's environmental diversity to study ER_{wc} across conditions found in the Columbia River basin. Our goal is to generate knowledge of ER_{wc} that could be transferable across the Columbia River basin, and potentially beyond. Our specific objectives were to 1) estimate the magnitude of ER_{wc} across the Yakima River basin during baseflow conditions; 2) investigate the relative importance of contributions from ER_{wc} to ER_{tot} through comparisons to published literature values of ER_{wc} and ER_{tot} from rivers beyond the Yakima River basin; and 3) investigate how ER_{wc} is organized spatially and with respect to environmental conditions to estimate the primary drivers of spatial variability in ER_{wc}. To test the transferability of study results to catchments throughout the Columbia River basin, we used cluster analysis to group catchments in the Columbia River basin into six classes sharing similar landscape characteristics using key biophysical and hydrological attributes selected from readily available spatial datasets. We collected water chemistry samples and measured ER_{wc} using a modified semi-*in situ* dark bottle incubation at field sites during low flow conditions during the summer of 2021. We then ran a multiple linear regression model using watershed characteristics and surface water chemistry to determine which explanatory variables best explained spatial variation in ER_{wc} across the Yakima River basin. Addressing these objectives indicated that across biomes, land use, etc., ER_{wc} in the Yakima River basin is similar to ER_{wc} in other basins and is likely a very small fraction of ER_{tot}, but variation in ER_{wc} is nonetheless well-explained by watershed, physical, and chemical conditions.

https://doi.org/10.5194/egusphere-2023-3038
Preprint. Discussion started: 15 January 2024

2 Methods

2.1 Methods Overview

We grouped all catchments in the Columbia River basin into six classes sharing similar landscape characteristics using key biophysical and hydrological attributes selected from readily available spatial datasets. We used this information to select field sites across six Strahler stream orders in the Yakima River basin spanning a wide range of land cover types and physical settings. To estimate the magnitude of ER_{wc} across the basin and investigate how ER_{wc} is organized spatially and with respect to environmental conditions, we collected surface water chemistry samples and measured ER_{wc} using dark bottle incubations at field sites during summer baseflow conditions in 2021 (i.e., the 2021 "Spatial Study" sampling event). To see how water column respiration rates in the Yakima River basin compared to rates observed in streams and rivers across the CONUS and around the world, and how the magnitude of ER_{wc} contributions to ER_{tot} may vary around the Yakima River basin, we also compared ER_{wc} observed in the basin against ER_{wc} and ER_{tot} published values found in the literature. We then used multiple linear regression to evaluate the nature of the relationship between ER_{wc} and Strahler stream order, drainage area, stream temperature, surface water chemistry, and the number of OM transformations and determine the primary drivers of ER_{wc} throughout the Yakima River basin. All analyses were performed using R Statistical Software (v4.2.0) (R Core Team, 2022). All data generated from the sampling study, including data not evaluated in this manuscript, and R scripts to run the statistical analyses for this study, are publicly available (Fulton et al., 2022; Grieger et al., 2022; Kaufman et al., 2023) (see Code and Data Availability section for more details on how to access these datasets).

2.2 Watershed characterization and site selection

The Yakima River basin is one of four major watersheds draining the Columbia River basin and is located entirely within the state of Washington, USA. The basin is roughly 16,000 km^2 and spans forested mountainous regions in the west to arid valleys and plains in the east (Fig 1a). The basin has a diversity of land covers and land uses dominated by dry rangeland, forest, and agriculture (Fig 1b). Annual precipitation ranges from 250 cm in the west to 25 cm in the east.

To test the transferability of study results to catchments throughout the Columbia River basin, we strategically selected sampling sites in the Yakima River basin based on their biophysical characteristics. This was done by first grouping all USGS National Hydrography Dataset Plus Version 2.1 (NHDPlusV2.1) catchments (U.S. Geological Survey, 2019b) in the Columbia River basin (n = 181,531) into six classes sharing similar landscape characteristics using cluster analysis. To capture the variability in hydrologic settings found across the Columbia River basin, we then selected multiple sites within each of the six Columbia River basin classes. We selected 16 key biophysical and hydrological attributes as input variables to the cluster analysis, including climate, vegetation structure and function, topography, and wildfire potential (Table S1). Existing, readily available geospatial data came from multiple sources including NASA Moderate Resolution Imaging Spectroradiometer (eMODIS) Remote Sensing Phenological (RSP) data (U.S. Geological Survey, 2019a); NASA MODIS land cover type (Friedl and Sulla-Menashe, 2019); NASA MODIS normalized difference vegetation index (NDVI), fraction of photosynthetically active radiation (FPAR, %), and leaf area index (LAI, $m^2\ m^{-2}$) (Myneni et al., 2015); NASA MODIS total evapotranspiration (ET, kg $H_2O\ m^{-2}\ d^{-1}$) (Running et al., 2017); NASA MODIS terrestrial net primary productivity (NPP, kg C $m^{-2}\ y^{-1}$) and terrestrial net ecosystem productivity data (NEP, kg C $m^{-2}\ y^{-1}$) (Running and Zhao, 2019); PRISM precipitation data (https://www.prism.oregonstate.edu/); NHDPlusV2.1 stream length and catchment boundaries (U.S. Geological Survey, 2019b); USGS National Elevation Dataset (NED) 1/3 Arc-Second Digital Elevation Model topography data (http://nationalmap.gov/elevation.html); USFS Wildfire Hazard Potential (WHP)

https://doi.org/10.5194/egusphere-2023-3038
Preprint. Discussion started: 15 January 2024

data (Dillon, 2018); and Landscape Fire and Resource Management Planning Tools (LANDFIRE) existing vegetation percent cover (%) and height (m) data (Dillon and Gilbertson-Day, 2020).

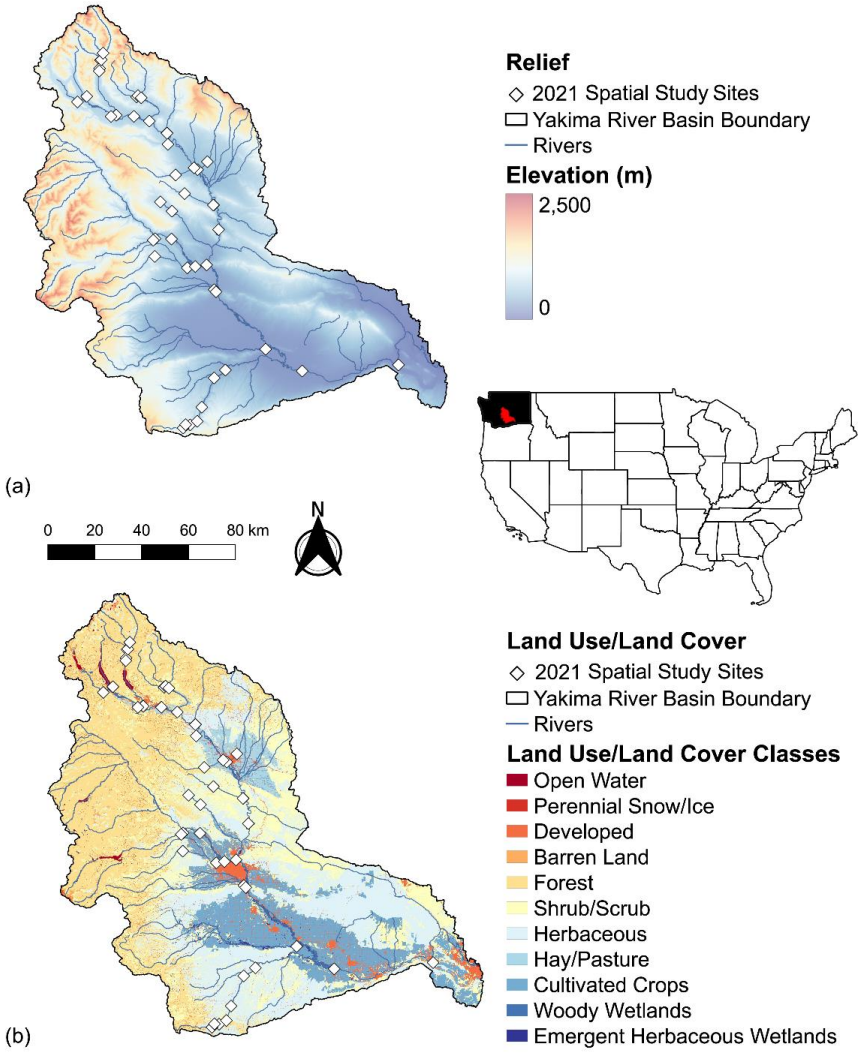

Figure 1. Yakima River basin study area, Washington, USA. (a) Map of land use/land cover classes in the Yakima River basin. (b) Relief map of the Yakima River basin. The highlighted red area within the state of Washington (shaded in black) shown in the inset map highlights the location of the Yakima River basin relative to the CONUS. The maps were generated by Brieanne Forbes using the Free and Open Source QGIS (v. 3.16.1 and v. 3.26.0). Map data include catchment boundaries and hydrography from the National Hydrography Dataset Plus (NHDPlusV2.1) (U.S. Geological Survey, 2019b), 30 m elevation data from the National Elevation Dataset (http://nationalmap.gov/elevation.html), and 2016 land use/land cover data from the National Land Cover Dataset (https://www.mrlc.gov).

https://doi.org/10.5194/egusphere-2023-3038
Preprint. Discussion started: 15 January 2024

We used a k-means clustering algorithm (R stats::kmeans function) to group NHDPlusV2.1 catchments with like properties using as input the normalized, statistical moments (minimum, maximum, mean, and standard deviation (SD)) for 70 geospatial variables within each NHDPlusV2.1 catchment (Table S1). To calculate statistical moments for each variable, we summarized geospatial data types at the NHDPlusV2.1 catchment level using two different methods: zonal statistics for continuous raster data and tabulation for vector data. Zonal statistics calculate statistical moments by individual catchment polygon. Tabulation calculates total length or area of a particular vector feature within each individual catchment polygons. We evaluated 13 different sets of variable-statistical moment combinations for use in the cluster analysis and selected variable set 8, which included the zonal mean and zonal SD for 70 variables (n = 140) (Table S2). Once the data for variable set 8 were summarized at the NHDPlusV2.1 catchment level, we calculated z-scores (z) for each geospatial variable as:

$$z = \frac{(X_{k,i} - \bar{X}_{k,i-n})}{SD_{k,i-n}} \quad (1)$$

where X = observed value for parameter k in the i_{th} NHDPlusV2.1 catchment, n = total number of NHDPlusV2.1 catchments in the Columbia River basin, $\bar{X}_{k,i-n}$ = the global mean of observed values for parameter k across the population of i−n NHDPlusV2.1 catchments in the Columbia River basin, and $SD_{k,i-n}$ = global standard deviation for parameter k across the population of i−n NHDPlusV2.1 catchments. Resultant z-scores for variable set 8 were fed into the k-means classifier, which iteratively adds each catchment to one of n clusters, with n being set by the user (n = 15, this study), using Euclidean distance to minimize within-cluster distance and maximize between-cluster distance. We ran multiple iterations of the cluster analysis using 2–15 clusters using the mean and SD of all variables. To visualize the reduction in within-cluster variation between iterations 1–15, we generated elbow plots by plotting the Within Cluster Sum of Squares (WCSS) value against the total number of catchments in a cluster and selected six clusters as the suitable number of clusters that minimized map visual complexity enough to guide manual site selection while maintaining a level of variation in key biophysical and hydrological variables representative of the Columbia River basin. Clusters 1 and 3–6 were categorized according to tree height, precipitation, and elevation (Table 1 and Table S3). Cluster 2 was categorized as "Water dominated" and was not used for selecting sites. Cluster analysis results were then used to guide the selection of 47 field sites distributed across Strahler stream orders 2–7 (the highest order stream in the Yakima River basin) that spanned the basin and captured the variation in biophysical and hydrologic parameters represented by clusters 1 and 3–6 (Fig S1). First order and other non-perennial streams were not sampled due to the lack of flow during summer baseflow or baseflows were too low to support sampling. We attempted to include logistical considerations in model-based site selection, but this task proved impractical and field-scouting trips were needed to refine site selections. Day-of-sampling changes to the sampling plan were made on-the-fly when the Schneider Springs Fire started on the Okanogan-Wenatchee National Forest. Fire activity and road closures restricted access to a large portion of the Yakima River basin, primarily in the Tieton River and American River watersheds located in the midwestern portion of the basin.

Table 1. Cluster analysis results characterizing NHDPlusV2.1 catchments across the Columbia River basin and Yakima River basin with similar biophysical and hydrologic characteristics and the number and percentage of sites in each basin.

Cluster	Name	CRB Drainage Area	YRB Drainage Area	YRB Sites Per Cluster	Percent YRB Sites Per Cluster
1	**Tree dominated high elevation mesic**	23%	27%	9	19%
2	**Water dominated**	3%	2%	0	0%
3	**Tree dominated high elevation hydric**	7%	2%	2	4%
4	**Shrub-steppe middle elevation xeric**	25%	28%	10	21%
5	**Tree dominated middle elevation mesic**	17%	17%	13	28%

https://doi.org/10.5194/egusphere-2023-3038
Preprint. Discussion started: 15 January 2024

6	**Tree dominated middle elevation xeric**	24%	23%	13	28%

"CRB Drainage Area" is the percentage of the total drainage area of the Columbia River basin that was classified in each cluster. "YRB Drainage Area" is the percentage of the total drainage area of the Yakima River basin that was classified in each cluster. "YRB Sites Per Cluster" is the total number of field sites in the Yakima River basin (*n* = 47) located in each cluster. "Percent YRB Sites Per Cluster" is the percentage of the total number of sampling sites in the Yakima River basin located in each cluster.

2.3 Water column respiration data collection

We measured ER_{wc} (mg O_2 L^{-1} d^{-1}) in triplicate for 2 h at each site between 30 August and 15 September 2021, using a modified "semi-*in situ*" dark bottle incubation water column metabolism approach (Genzoli and Hall 2016) (Fig 2). DO sensors (miniDOT Logger; Precision Measurement Engineering, Inc.; Vista, CA, USA) recorded DO concentration (mg L^{-1}) and temperature (°C) at 1-min intervals in 2-L dark bottles (Nalgene™ Rectangular Amber HDPE bottles; ThermoFisher Scientific; Waltham, Massachusetts, USA) (Fulton et al., 2022). Bottle necks were slightly widened (1 to 2 mm) using a drill press and a hole saw to accommodate the diameter of the DO sensor. A small, battery-powered mixing device (i.e., toy boat motor propellor) was placed inside each bottle to mix the water samples throughout the duration of the incubation (Underwater Motor, Item Number 7350; Playmobil; Shanghai, China; rechargeable AA NiMH battery; Amazon; Seattle, Washington, USA). Bottles remained filled with river water throughout the sampling period to minimize the potential bias on ER_{wc} caused by the diffusion of atmospheric oxygen into bottle micropores and the subsequent re-release of that oxygen into river water samples during deployment.

At the start of each sampling day, DO sensors and all sampling equipment were placed in a cooler with blue ice packs to keep them cool and minimize the time needed at each site for the sensors to equilibrate with the similarly cool river water temperatures. Bottles were emptied upon arrival at each site, rinsed three times with river water, and filled with river water by wading as close to the thalweg as possible, submerging the bottles below the river surface, and rolling them 360 degrees while held upright underwater to ensure no air bubbles were present in the bottles (Fig 2a). After filling a second cooler with river water and placing it in the shade on the streambank, the bottles were placed in the cooler and secured to the bottom using pre-applied Velcro strips to keep the bottles upright and allowed to equilibrate for 20 min. Following the 20-min equilibration period, the bottles were emptied and re-filled with fresh river water as described above, the battery-powered mixing device and DO sensor were gently inserted (sensor face-up) in the bottles to minimize trapping air bubbles in the bottles, the bottles were capped underwater, and returned to the cooler (Fig 2a). We ran the incubation test for 2 h, replenishing river water in the cooler every 20 min to maintain *in situ* temperature.

https://doi.org/10.5194/egusphere-2023-3038
Preprint. Discussion started: 15 January 2024

Figure 2. Modified semi-*in situ* dark bottle incubation method and example study sites. (a) Underwater photograph of DO sensor being inserted into incubation bottle filled with river water and mixing device. Right panels emphasize the diversity of environmental settings covered in this study. (b) West Fork Teanaway River (site S20R), Kittitas County, Washington, 02 September 2021. Site 20R is classified as a mesic, high elevation site dominated by tree canopy (Cluster 1; see Table 1, Table S3, and Fig S1a). (c) Yakima River at Mabton (site T02), Yakima County, Washington, 07 September 2021. Site T02 is classified as a mesic, middle elevation site dominated by tree canopy (Cluster 5; see Table 1, Table S3, and Fig S1a). Poor air quality evident in the photograph is due to significant smoke impacts from the Schneider Springs Fire burning ~105 km northwest of site T02.

2.4 Surface water chemistry sample collection and analysis

Filtered surface water samples were collected in triplicate for each site for dissolved inorganic C (DIC, mg L^{-1}); dissolved organic C (DOC, mg L^{-1}); ions, including nitrate (NO_3-N, mg L^{-1}); and OM chemistry (Grieger et al., 2022). Samples were collected using a 50-mL syringe and filtered into 40 mL amber glass vials (ThermoScientific™ Amber Clean Snap Vials (DOC, NO_3-N, and OM) or Amber Clean Snap Vials with 0.125 in Septa (DIC); Thermo Fisher Scientific; Waltham, Massachusetts, USA) using a 0.22 µm sterivex filter (MilliporeSigma™ Sterivex™ Sterile Pressure-Driven Devices; MilliporeSigma™; Burlington, Massachusetts, USA). DIC samples were collected using a sterivex filter equipped with an 18 g needle (DIC only) (BD General Use and PrecisionGlide Hypodermic Needles; Becton, Dickinson and Company; Franklin Lakes, NJ, USA). Samples collected for ion analysis (including NO_3-N) were filtered using a 0.22 um sterivex filter into a 15 mL conical tube (Olympus). Samples collected for OM chemistry were filtered into pre-acidified (85 % phosphoric acid, H_3PO_4) amber vials (Grieger et al., 2022). Filter and filter+needle assemblies were rinsed once by pushing 5 mL of river water through the filter prior to collecting the first sample and removed before pulling each fresh volume of water. Each triplicate sample was collected while pushing a final 50 mL of river water through the syringe and then capped with a surface tension dome of water to ensure no headspace. DIC samples were

https://doi.org/10.5194/egusphere-2023-3038
Preprint. Discussion started: 15 January 2024

collected by placing the sterile needle inside the vial and pushing three vial-volumes of river water (~150 mL) slowly through the syringe to prevent the introduction of air bubbles to the sample while allowing the vials to overflow continuously. Five mL of uncollected water were pushed through the syringe between samples to ensure independent samples. Samples were collected from 50 % of the water column depth in sample containers using nitrile gloves and sterile sampling techniques. One unfiltered grab sample for total suspended solids (TSS, mg L^{-1}) was collected using a pre-washed 2-L amber bottle (Nalgene™ Rectangular Amber HDPE Bottles; ThermoFisher Scientific; Waltham, Massachusetts, USA). TSS bottles were rinsed three times with river water prior to sample collection. All samples were stored on ice in the field and then refrigerated at 4° C before shipping for analysis at the Pacific Northwest National Laboratory (PNNL) Marine and Coastal Research Laboratory in Sequim, Washington (NO_3-N, DOC, and DIC) and PNNL Biological Sciences Facility Laboratory in Richland, Washington (TSS and OM characterization). TSS samples were analyzed within one week of collection, DOC concentrations were measured within two weeks of collection, DIC content was measured within one month of collection, ion samples were frozen upon arrival at the laboratory and NO_3-N content was measured within two months of collection, and OM samples were immediately frozen (−20 °C) upon receiving.

DOC was measured as non-purgeable organic C (NPOC), which removes inorganic and volatile C species by purging with gas after in-line acidification, after which the sample is converted to carbon dioxide (CO_2) via catalytic combustion. DIC was measured by bubbling samples in 25 % H_3PO_4 and CO_2 was detected via nondispersive infrared detection (NDIR). CO_2 generated via DOC and DIC methods were then detected via chemiluminescence on a Shimadzu TOC-L Total Organic Carbon Analyzer. NO_3-N was measured via ultraviolet (UV) absorbance on a Thermo Scientific Dionex ICS-6000 DP. Visual checks of calibration curves, samples, blanks, and check standard peaks were performed before exporting data. Concentrations below the limit of detection (LOD) of the instrument, or below the standard curve, were flagged (Grieger et al., 2022). The coefficient of variation (CV) for each replicate set was calculated. Sets with CV of 30 % or higher were flagged and the outlier sample was identified by calculating the distance between each of the replicate samples. Replicates with the highest distance to the other two replicates were flagged as outliers and removed from the analysis. Parameter mean values for each site were then calculated from the remaining replicates and input as predictor variables in the multiple linear regression (Sect. 2.7).

TSS samples were filtered in the laboratory through a pre-weighed and pre-combusted 4.7 cm, 0.7 µm GF/F glass microfiber filter (Whatman™ glass microfiber filters, Grade 934-AH®; MilliporeSigma; Burlington, Massachusetts, USA). After water filtration, the filter and filtration apparatus were rinsed with 30 mL of ultrapure Milli-Q water (Milli-Q® IQ Water Purification System; MilliporeSigma; Burlington, Massachusetts, USA) to ensure that all residue was captured by the filter. The filter was placed in foil and oven dried overnight at 45° C. The filter was allowed to cool in a desiccator prior to weighing. TSS (mg L^{-1}) was calculated as the difference between the weight (mg) of the filter before and after filtration of the water sample divided by the volume of water filtered (L).

2.5 OM chemistry via ultra-high resolution mass spectrometry and biochemical transformations

Organic matter chemistry was characterized via ultra-high resolution mass spectrometry using a 12 Tesla (12T) Bruker SolariX Fourier transform ion cyclotron resonance mass spectrometer (FTICR-MS) at the PNNL Environmental Molecular Sciences Laboratory in Richland, Washington, following methods described in Garayburu-Caruso et al. (2020b). Briefly, samples were thawed in the dark at 4° C overnight. We used the DOC concentrations to normalize the DOC concentration of the sample to 1.5 mg C L^{-1}. Normalized samples were acidified to pH 2 using 85 % H_3PO_4 and were then subjected to solid phase extraction (SPE) using Bond Elut PPL cartridges (sorbent modified with a proprietary nonpolar surface; Agilent; Santa Clara, CA, USA) following

https://doi.org/10.5194/egusphere-2023-3038
Preprint. Discussion started: 15 January 2024

protocols employed by Dittmar et al. (2008). Extracted samples were run in the FTICR-MS with a standard electrospray ionization source in negative mode. Data were collected with an ion accumulation time of 0.08 seconds. BrukerDaltonik Data Analysis version 4.2 was used to convert raw spectra to a list of molecular compound mass-to-charge ratios (m/z) with a signal-to-noise ratio (S/N) threshold set to 7 and absolute intensity threshold to the default value of 100. Peaks were aligned (0.5 ppm threshold) and molecular formula were assigned using the Formularity software with S/N > 7 and mass measurement error < 0.5 ppm (Tolić et al., 2017). The Compound Identification algorithm takes into consideration the presence of C, H, O, N, S, and P and excludes other elements. Aligned and calibrated data was further processed using ftmsRanalysis (Bramer et al., 2020). Replicate samples were merged into one site where peaks in a sample were retained if they were present in at least one of the replicates. OM biochemical transformations were inferred following methods previously employed by Garayburu-Caruso et al. (2020b). In summary, we calculated pairwise mass differences between every peak in a sample regardless of molecular formula assigned and compared that mass difference to a list of 1,255 molecular masses associated with commonly observed biochemical transformations (Table S4). Biochemical transformations allow you to infer the number of times a specific molecule is gained or lost. For example, if a mass difference between two peaks corresponded to 128.095, that would correlate to the loss or gain of the amino acid lysine (see Table S4). We further calculated the total number of OM transformations per site and the total number of OM transformations normalized by the number of peaks present in the site (i.e., "normalized OM transformations").

2.6 DO sensor data cleaning, processing, and analysis

We extracted the raw DO concentration (mg O_2 L^{-1}) and temperature (°C) sensor data for each site and plotted DO and temperature against incubation time for each set of triplicate incubations (n = 141). The plots were visually inspected to a) confirm that temperature sensors were at equilibrium with the river temperature when the 2-h incubation test period began and b) identify data gaps, outliers, and other data anomalies. Following the visual inspection of plots, we removed the first and last 5 min of the 2-h incubation time series data to account for data anomalies due to emptying and refreshing river water in the bottles at the beginning and end of the incubation period. Sensor data distributions were also evaluated using violin plots for each site.

Water column respiration rates for individual triplicate incubation samples were calculated as the slope of the linear regression model (R stats::lm function) fit to the DO sensor data (mg O_2 L^{-1} min^{-1}), which was converted to daily units (mg O_2 L^{-1} d^{-1}) using Eq. (2):

$$ER_{wc} = (m_{DO})(t) \quad (2)$$

Where m_{DO} = the slope of the regression line (mg O_2 L^{-1} min^{-1}) and t = number of minutes in a day (min d^{-1}). Only sample observations with a normalized root mean square error (NRMSE) ≤ 0.01 were used for further analysis (Shcherbakov et al., 2013) and all triplicate samples except one at site T03 (Yakima River at Union Gap) met the NRMSE criteria. Mean ER_{wc} for each site and the global mean and variance were calculated from the remaining samples (n = 140) (R stats::lme4 package) (Bates et al., 2015). More than one-third of ER_{wc} values were slightly positive (i.e., $ER_{wc} > 0$). Although positive respiration rates are biologically unrealistic, and values greater than 0 mg O_2 L^{-1} d^{-1} but less than 0.5 mg O_2 L^{-1} d^{-1} are difficult to distinguish from zero (Appling et al., 2018b), we retained positive ER_{wc} values.

https://doi.org/10.5194/egusphere-2023-3038
Preprint. Discussion started: 15 January 2024

2.7 Relationship of water column respiration rates to watershed characteristics and surface water chemistry

We evaluated the relationship between ER_{wc} and watershed characteristics and surface water chemistry using multiple linear regression models (R stats::lm function) to establish which explanatory variables best explained spatial variation in ER_{wc} across the Yakima River basin. Explanatory variables hypothesized to control ER_{wc} were selected a priori. Variables included in the full model were drainage area, Strahler stream order, stream temperature, NO_3-N, DOC, DIC, TSS, number of OM transformations, and normalized number of OM transformations. Drainage area (km^2) was defined as the total upstream drainage area from each site and was extracted for each site from the USGS NHDPlusV2.1 stream database (https://www.epa.gov/waterdata/get-nhdplus-national-hydrography-dataset-plus-data) using site latitude and longitude (Wieczorek et al., 2018). Stream order for each site was extracted as the reach attribute "StreamOrde" from the NHDPlusV2.1 stream database, which is a modified version of Strahler stream order (Mckay et al., 2012). We observed that several model input variables had skewed distributions. To improve normality, we $\log_{10}$ transformed all variables. The best fit model was determined using stepwise forward selection (R stats::step function). Akaike Information Criterion corrected for small sample size (AIC_c) was used as the model selection criterion, with models having $\Delta AIC_c < 2$ equally likely to describe the data (Burnham and Anderson, 2007; Aho et al., 2014).

2.8 Comparison to published water column respiration rates

To contextualize the magnitude of observed water column respiration rates in the Yakima River basin, we compared our results to published literature values of ER_{wc} and ER_{tot}. Areal estimates of ER_{wc} (g O_2 m^{-2} d^{-1}) for temperate and tropical streams and rivers (n = 25) were first converted to volumetric units (this study; mg O_2 L^{-1} d^{-1}) using standard unit conversions and then multiplied by 1/depth (m^{-1}) using same-day depth data for each reach studied or same-day depth data from related studies when available. We also compared our ER_{wc} values to daily reach-averaged estimates of ER_{tot} (n = 490,907) for 356 rivers and streams across the CONUS by using the Appling et al. (2018c) dataset. For comparison with our ER_{wc} values, we first converted Appling et al. (2018b, 2018c) ER_{tot} areal units to volumetric units as described above and then calculated the mean value for each site (n = 356) by summing daily predictions and dividing by the number of observations for each site. Fifteen sites had positive ER_{tot} values (i.e., $ER_{tot} > 0$), which—as mentioned previously (see Sect. 2.6)—is a biologically unrealistic outcome (Appling et al., 2018b). For our comparative analysis, we culled potentially problematic sites from the Appling et al. (2018c) dataset by matching site IDs with the StreamPULSE sites (n = 222) and keeping sites common to both datasets, which resulted in a total of 208 sites used in this study. StreamPULSE sites are a subset of sites from the Appling et al. (2018c, 2018b) dataset for 222 rivers across the CONUS created by Bernhardt et al. (2022) through a robust data quality analysis to remove sites potentially affected by process or observation error.

3 Results and discussion

3.1 Water column respiration rates were slow and may contribute little to reach-scale ecosystem respiration

DO sensor time series datasets (mg O_2 L^{-1}) from the triplicate incubation bottles used at two distinctly different example sites—West Fork Teanaway River (site S20R; Fig 2b) and Yakima River at Mabton (site T02; Fig 2c)—show how consistent DO and temperature measurements were across replicates (Fig 3). The linear regression models for each triplicate set of DO sensor measurements were well fit to the data and all sites except one (site T03, Yakima River at Union Gap) met the criteria for NRMSE ≤ 0.01 (Fig 3). Comparison of triplicate sample ER_{wc} rates (mg O_2 L^{-1} d^{-1}) showed that within-sample variation was small ($\bar{s}$ = 0.004 mg O_2 L^{-1} d^{-1}), indicating that the method we used consistently generated precise data (Bórquez-López et al., 2020) for all streams sampled throughout the Yakima River basin (Fig 4). ER_{wc} rates ranged from −0.11–0.03 mg O_2 L^{-1} d^{-1}, with a median

https://doi.org/10.5194/egusphere-2023-3038
Preprint. Discussion started: 15 January 2024

value of −0.01 mg O_2 L^{-1} d^{-1} (global mean: −0.01, standard error = 0.003 mg O_2 L^{-1} d^{-1}), indicating relatively little consumption of DO within the water column (Fig 5a). Thirteen sites had at least one individual replicate incubation where ER_{wc} > 0.0 mg O_2 L^{-1} d^{-1}. Positive ER_{wc} values shown in Fig 4 likely indicate that true ER_{wc} values were too small to overcome instrument noise (i.e., values were indistinguishable from 0). The distribution of ER_{wc} was left-skewed (skewness = −2.69) with few outliers, illustrating how consistently slow (i.e., very small negative values) observed ER_{wc} rates were throughout the Yakima River basin during baseflow conditions (Fig 5a).

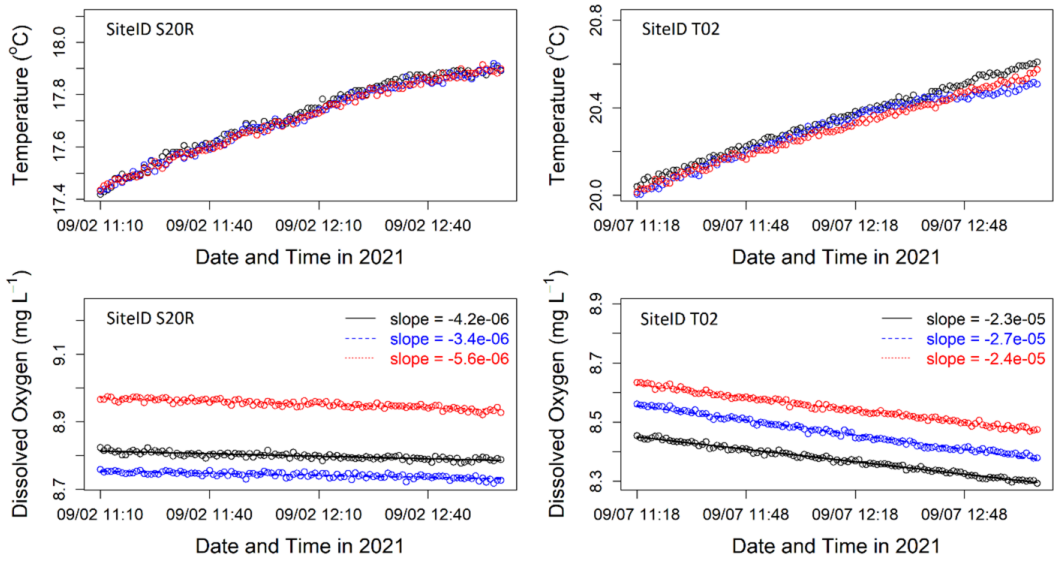

Figure 3. Example triplicate incubation bottle dissolved oxygen (DO) sensor time series data and linear regression models fit to the data for two sites in the Yakima River basin in different environmental settings. Left: West Fork Teanaway River (site S20R), Kittitas County, Washington. Right: Yakima River at Mabton (site T02), Yakima County, Washington. The red, blue, and black circles are raw sensor measurements logged on a 1-min time interval for each replicate bottle. Temperature data (°C) are shown in the top two panels. DO data (mg L^{-1}) are shown in the lower two panels and the red, blue, and black lines are the regression lines fit to each data set. The slope (mg O_2 L^{-1} min^{-1}) is provided for each regression model. The regression models were well fit to the data with a normalized root mean square error (NRMSE) ≤ 0.01. Water column respiration rates (ER_{wc}) for each site were calculated as the mean slope (converted to daily units using Eq (2); mg O_2 L^{-1} d^{-1}) of the three regression models.

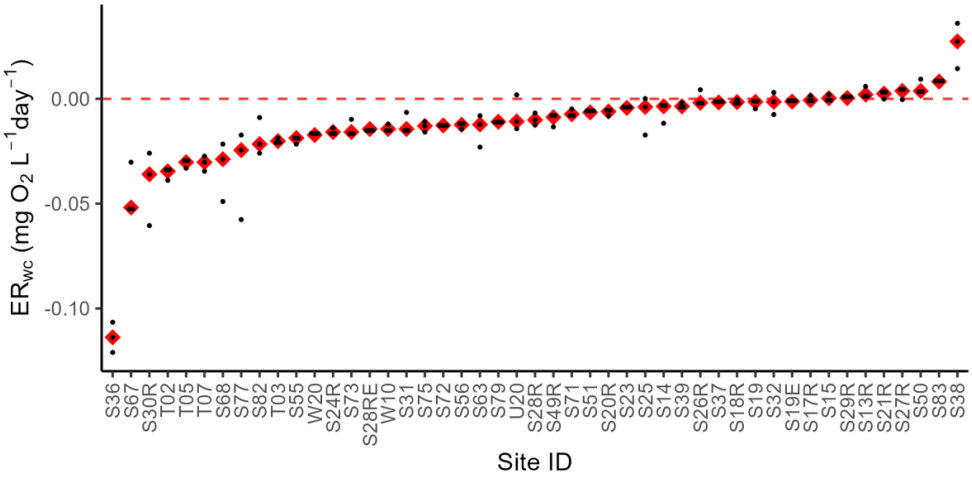

https://doi.org/10.5194/egusphere-2023-3038
Preprint. Discussion started: 15 January 2024

Figure 4. Dot plot comparison of the mean water column respiration rates for the triplicate sample incubations at each site (n = 141). Black dots represent water column respiration rates (ER_{wc}, mg O_2 L^{-1} d^{-1}) from individual replicates. Red diamonds represent the mean ER_{wc} at each site. More negative ER_{wc} rates indicate greater oxygen consumption. Positive ER_{wc} rates are a biologically unrealistic outcome and likely indicate true oxygen consumption rates were too small to overcome instrument noise.

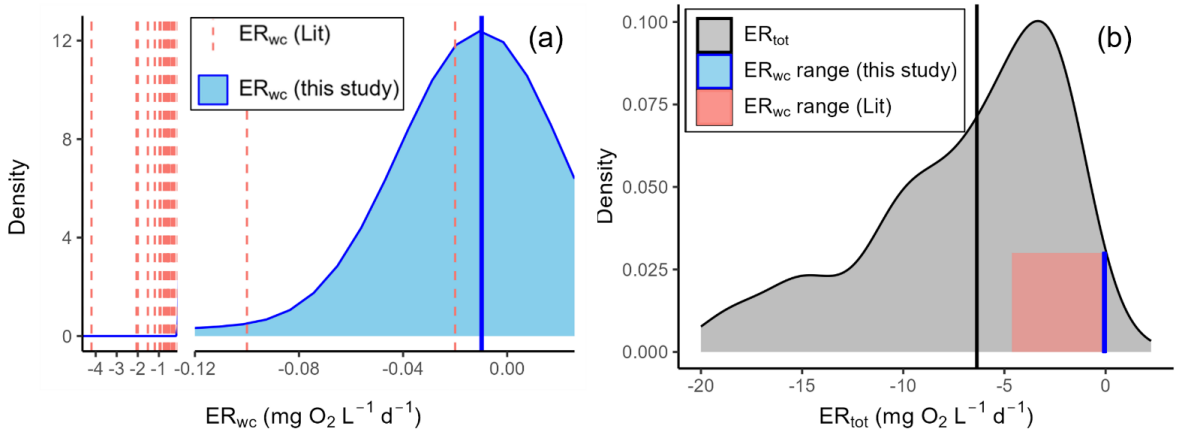

Figure 5. Kernel density plots and ranges of water column respiration data from the Yakima River basin (this study), published water column respiration rates from the literature, and reach-scale ecosystem respiration estimated by Appling et al. (2018b, 2018c). (a) The distribution of mean water column respiration values from this study (ER_{wc} (this study); n = 47) overlayed with published mean water column respiration values from the literature (ER_{wc} (Lit); n = 25). The vertical, solid blue line is the median ER_{wc} observed in the Yakima River basin (−0.01 mg O_2 L^{-1} d^{-1}). The dashed vertical red lines are the published mean ER_{wc} values from studies in rivers across the CONUS and the Amazon River basin (Table 2). (b) The distribution and range (−77.63–1.34 mg O_2 L^{-1} d^{-1}) of mean daily reach-averaged ecosystem respiration rates (ER_{tot}, mg O_2 L^{-1} d^{-1}) for rivers and streams across the CONUS estimated by Appling et al. (2018b, 2018c) and modified by Bernhardt et al. (2018) (n = 208) overlayed with the range and median values for ER_{wc} (this study) and ER_{wc} (Lit). The X-axis ranges from -20.00–1.34 mg O_2 L^{-1} d^{-1} for visualization purposes; only two sites fall outside the cutoff at -20.00 mg O_2 L^{-1} d^{-1}. The vertical solid black line is the median ER_{tot} value (−3.51 mg O_2 L^{-1} d^{-1}). The vertical blue and shaded red columns represent the range of ER_{wc} values for this study (−0.11–0.03 mg O_2 L^{-1} d^{-1}) and from published studies (−4.63–−0.02 mg O_2 L^{-1} d^{-1}), respectively (Table 2).

The values of ER_{wc} observed in our study are generally at the very slow end of the range of published literature values (Table 2). For example, ER_{wc} in the water column of the Amazon River and several large tributaries was measured in stationary (i.e., no mixing) and rotating (i.e., bottles were rotated at two different speeds to ensure mixing) incubation bottles (Ward et al., 2018). ER_{wc} rates in stationary incubation bottles were 10−30× higher than those measured in the Yakima River basin: ER_{wc} values ranged from −1.0–−2.9 mg O_2 L^{-1} d^{-1} (mean: −2.0 mg O_2 L^{-1} d^{-1}) (Ward et al., 2018). Furthermore, increased velocity in rotating bottles enhanced maximum ER_{wc} rates by ~2–3× compared to stationary bottles: rotating bottle ER_{wc} measurements ranged from −1.3–−6.1 mg O_2 L^{-1} d^{-1} (mean: −2.0 mg O_2 L^{-1} d^{-1}) and −2.6–−8.1 mg O_2 L^{-1} d^{-1} (mean: −4.2 mg O_2 L^{-1} d^{-1}) for bottles spun at 0.22 m s^{-1} and 0.66 m s^{-1}, respectively. Our approach used continuous mixers within each bottle and is likely similar to the rotational method of Ward et al. (2019), thereby avoiding artificially slow rates; however, ER_{wc} rates from our study were nonetheless substantially slower than the ER_{wc} rates measured in unmixed bottles of Amazon rivers (Ward et al., 2019). The very slow rates we observed demonstrate very small amounts of *in situ* respiration in the water column across the Yakima River basin. The relatively slow ER_{wc} values measured in the basin is further emphasized by comparison to additional literature values (Table 2). For example, Reisinger et al. (2021) measured ER_{wc} over a substantially larger range of values (min: −0.10, max: −4.63 mg O_2 L^{-1} d^{-1}) than in the Yakima River basin. Rivers in Reisinger et al. (2021) spanned 13 mid-sized turbid midwestern rivers and both clear and turbid western rivers across a gradient of turbidity levels and nutrient concentrations, which collectively had a median ER_{wc} value (−0.60 mg O_2 L^{-1} d^{-1}) that was 60× greater than the median ER_{wc} value observed in the Yakima River basin (−0.01 mg O_2

https://doi.org/10.5194/egusphere-2023-3038
Preprint. Discussion started: 15 January 2024

410 L^{-1} d^{-1}). However, while ER_{wc} rates in the Yakima River basin were slow, they were not outside the range of reported literature values. For example, 14 rivers in the Amazon River basin had slow ER_{wc} (−0.02–−0.96 mg O_2 L^{-1} d^{-1}) in a study by Ellis et al. (2012). ER_{wc} rates measured in the mainstem Amazon River near Manaus, Brazil, ranged from −0.05–−0.86 mg O_2 L^{-1} d^{-1} (Devol et al., 1995). Another study in the same year observed similarly slow water column respiration at nine sites along the Amazon River mainstem, with ER_{wc} rates ranging from −0.08–−0.77 mg O_2 L^{-1} d^{-1} (Quay et al., 1995). Lastly, relatively slow ER_{wc} values
415 were observed in the lower mainstem Amazon River during both during low water (−0.95 ± 0.10 mg O_2 L^{-1} d^{-1}) and high water periods (−1.52 ± 0.35 mg O_2 mg O_2 L^{-1} d^{-1}) (Gagne-Maynard et al., 2017).

Table 2. River ecosystem metabolism studies that measured water column respiration rates.

River	Description	ER_{wc}[a]	Source	Year
Amazon River	Amazon River mainstem near Manaus, Brazil	−0.27 ± 0.18 *(−0.05, −0.86)*	Devol et al.[b,c]	1995
Rivers in the Amazon Basin	Amazon River mainstem near Vargem Grande, Xibeco, Tupe, Jutica, Itapeua, Anori, Manacapuru, Sao Jose do Amatari, Paura, and Obidos during three cruises of the CAMREX project	−0.32 *(−0.08, −0.77)*	Quay et al.[b]	1995
Barro Branco River, southwestern Amazon Basin	Clear water river at the falling water stage	−0.02	Ellis et al.[b,d]	2012
Acre River, State of Amazonas, southwestern Amazon Basin	Whitewater river at low water stage	−0.96	Ellis et al.[b,d]	2012
Clear, whitewater, and blackwater rivers in the southwestern and central Amazon Basin	A subset of "small" rivers classified according to drainage area (km^2)	−0.22 ± 0.20	Ellis et al.[b,d]	2012
Clear, whitewater, and blackwater rivers in the southwestern and central Amazon Basin	A subset of "mid-sized" rivers classified according to drainage area (km^2)	−0.73 ± 0.12	Ellis et al.[b,d]	2012
Clear, whitewater, and blackwater rivers in the southwestern and central Amazon Basin	A subset of "large" rivers classified according to drainage area (km^2)	−0.11 ± 0.06	Ellis et al.[b,d]	2012
Klamath River, CA	Seiad site, the uppermost reach of the Klamath River	−0.58 ± 0.38	Genzoli and Hall[e]	2016
Klamath River, CA	Weitchpec reach, middle reach of the Klamath River	−0.92 ± 0.75	Genzoli and Hall[e]	2016
Klamath River, CA	Turwar reach, the lowermost reach of the Klamath River located 9 km upstream of the mouth	−0.38 ± 0.16	Genzoli and Hall[e]	2016
Amazon River mainstem	Average water column respiration rate measured across five sites on the mainstem Amazon River at high water	−0.95 ± 0.10	Gagne-Maynard et al.[f]	2017
Amazon River mainstem	Average water column respiration rate measured across five sites on the mainstem Amazon River at low water	−1.52 ± 0.35	Gagne-Maynard et al.[f]	2017
Amazon River, Tapajós River, and Xingu River	Varying mixtures of turbid Amazon River water and two lowland tributaries—the Tapajós and Xingu rivers spun at 0.66 m s^{-1}	−4.2 *(−2.6, −8.1)*	Ward et al.[g]	2018
Amazon River, Tapajós River, and Xingu River	Varying mixtures of turbid Amazon River water and two lowland tributaries—the Tapajós and Xingu rivers spun at 0.22 m s^{-1}	−2.0 *(−1.3, −6.1)*	Ward et al.[g]	2018
Amazon River, Tapajós River, and Xingu River	Varying mixtures of turbid Amazon River water and two lowland tributaries—the Tapajós and Xingu rivers spun at 0 m s^{-1}	−2.0 *(−1.0, −2.9)*	Ward et al.[g]	2018
East Fork, White River	Midwest CONUS	−2.06	Reisinger et al.[h]	2021
Manistee River	Midwest CONUS	−0.50	Reisinger et al.[h]	2021
Muskegon River	Midwest CONUS	−0.67	Reisinger et al.[h]	2021

https://doi.org/10.5194/egusphere-2023-3038
Preprint. Discussion started: 15 January 2024

St. Joe	Midwest CONUS	−0.52	Reisinger et al.[h]	2021
Tippecanoe River	Midwest CONUS	−0.57	Reisinger et al.[h]	2021
Buffalo Fork	Clear water in western CONUS	−4.63	Reisinger et al.[h]	2021
Snake River	Clear water in western CONUS	−0.60	Reisinger et al.[h]	2021
Green River, WY	Clear water in western CONUS	−0.10	Reisinger et al.[h]	2021
Henry's Fork	Clear water in western CONUS	−0.26	Reisinger et al.[h]	2021
North Platte River	Turbid water in western CONUS	−0.10	Reisinger et al.[h]	2021
Bear River	Turbid water in western CONUS	−0.76	Reisinger et al.[h]	2021
Green River at Ouray	Turbid water in western CONUS	−1.19	Reisinger et al.[h]	2021
Green River at Gray Canyon	Turbid water in western CONUS	−0.73	Reisinger et al.[h]	2021

[a] Volumetric ER_{wc} units in mg O_2 L^{-1} d^{-1}. To compare to ER_{wc} values in the Yakima River basin, given units for ER_{wc} values from the literature were converted to volumetric units using standard conversions (see footnotes b, e, f, g, and h) and depth data (as needed).
[b] ER_{wc} units given in µmole O_2 per hour (h^{-1}). Given units were converted by multiplying µmole O_2 by 0.022391 mg O_2 L^{-1} and by multiplying hours (h^{-1}) by 24 hours per day (h d^{-1}). Resultant ER_{wc} values were then multiplied by −1 to account for methodological differences in respiration rate calculations.
[c] ER_{wc} "...was calculated from the average oxygen difference between sample and poisoned control."
[d] ER_{wc} was determined as "...the rate of change between the initial and final replicates over the incubation period in µmole of O_2 L^{-1} h^{-1}."
[e] Given units (g O_2 m^{-2} d^{-1}) were divided by mean depth (m^{-1}) to convert to equivalent volumetric units used in this study (mg O_2 L^{-1} d^{-1}).
[f] Given units for ER_{wc} (g O m^{-3} d^{-1}) were equivalent to volumetric units used in this study (mg O_2 L^{-1} d^{-1}). Resultant ER_{wc} values were multiplied by −1 to account for methodological differences in respiration rate calculations.
[g] Given units for ER_{wc} (mg O_2 L^{-1} d^{-1}) were equivalent to volumetric units used in this study (mg O_2 L^{-1} d^{-1}). Resultant ER_{wc} values were multiplied by −1 to account for methodological differences in respiration rate calculations.
[h] Given units (g O_2 m^{-2} d^{-1}) were divided by mean depth (m^{-1}) to convert to equivalent volumetric units used in this study (mg O_2 L^{-1} d^{-1}). Resultant ER_{wc} values were then multiplied by −1 to account for methodological differences in respiration rate calculations.

The slow rates of ER_{wc} across the Yakima River basin lend credence to recent work on stream metabolism across the Yakima River basin and the broader Columbia River basin that focused on reactions occurring within and below the riverbed (Son et al., 2022). That is, the slow water column respiration rates indicate that ER_{wc} is likely a small component of ER_{tot} across the Yakima River basin during baseflow. While ER_{tot} estimates are not available across the Yakima River basin, ER_{wc} rates across the basin were very slow relative to ER_{tot} rates estimated by Appling et al. (2018c, 2018b) across the CONUS: the fastest ER_{wc} rate in the Yakima River basin (−0.11 mg O_2 L^{-1} d^{-1}) was slower than every ER_{tot} rate estimated for 208 CONUS rivers and streams (range: −77.63–1.34 mg O_2 L^{-1} d^{-1}) (Fig 5b). The sample distribution for CONUS ER_{tot} was left-skewed (skewness = −2.94), and the median value of −6.36 mg O_2 L^{-1} d^{-1} is ~630× greater than the median ER_{wc} rates (−0.01 mg O_2 L^{-1} d^{-1}) observed in the Yakima River basin (Fig 5b).

3.2 ER_{wc} is well-explained by watershed characteristics and surface water chemistry

While our measured rates of ER_{wc} were slow relative to published values of both ER_{wc} and ER_{tot}, regression model results show that ER_{wc} nonetheless varied spatially across the Yakima River basin and was well explained by chemical and physical water quality parameters. When provided with drainage area, Strahler stream order, temperature, NO_3-N, DOC, DIC, TSS, total number of OM transformations, and normalized OM transformations, NO_3-N, DOC, and temperature were retained in the multiple regression model; these three variables together explained 41.5 % of the total variation in ER_{wc} (Table 3). Our results show that ER_{wc} increased (i.e., was faster) with increasing NO_3-N, increasing DOC, and increasing temperature (Fig 6). Faster ER_{wc} with increasing NO_3-N, DOC, temperature in the Yakima River basin is unsurprising since nutrients, DOC, and temperature can drive variation in stream metabolism (Honious et al., 2021; Hornbach, 2021; Bernot et al., 2010; Nakano et al., 2022). An increase with NO_3-N may not always we expected, however, as Reisinger et al. (2021) found that ER_{wc} was faster with more NH_4^+ but slower with more NO_3-N. This finding suggests that additional work is needed to unravel the joint influences of different N species on ER_{wc}.

https://doi.org/10.5194/egusphere-2023-3038
Preprint. Discussion started: 15 January 2024

Table 3. Multiple linear regression model results for the best fit model predicting water column respiration across the Yakima River basin.

Predictor Variable	Parameter Estimate	Standard Error	τ value	p-value
Intercept	4.28×10^{-2}	3.76×10^{-2}	1.137	2.62×10^{-1}
$\log_{10}(NO_3\text{-N})$	-1.27×10^{-2}	4.50×10^{-3}	−2.823	7.32×10^{-3}
$\log_{10}(DOC)$	-2.49×10^{-2}	1.41×10^{-2}	−1.766	8.49×10^{-2}
$\log_{10}(temperature)$	-1.58×10^{-2}	3.16×10^{-2}	−1.764	8.52×10^{-2}

The best fit model (R^2 = 41.5) was determined using step-wise forward selection with Akaike's Information Criterion adjusted for small sample size (ΔAIC_c) as our model selection criterion.

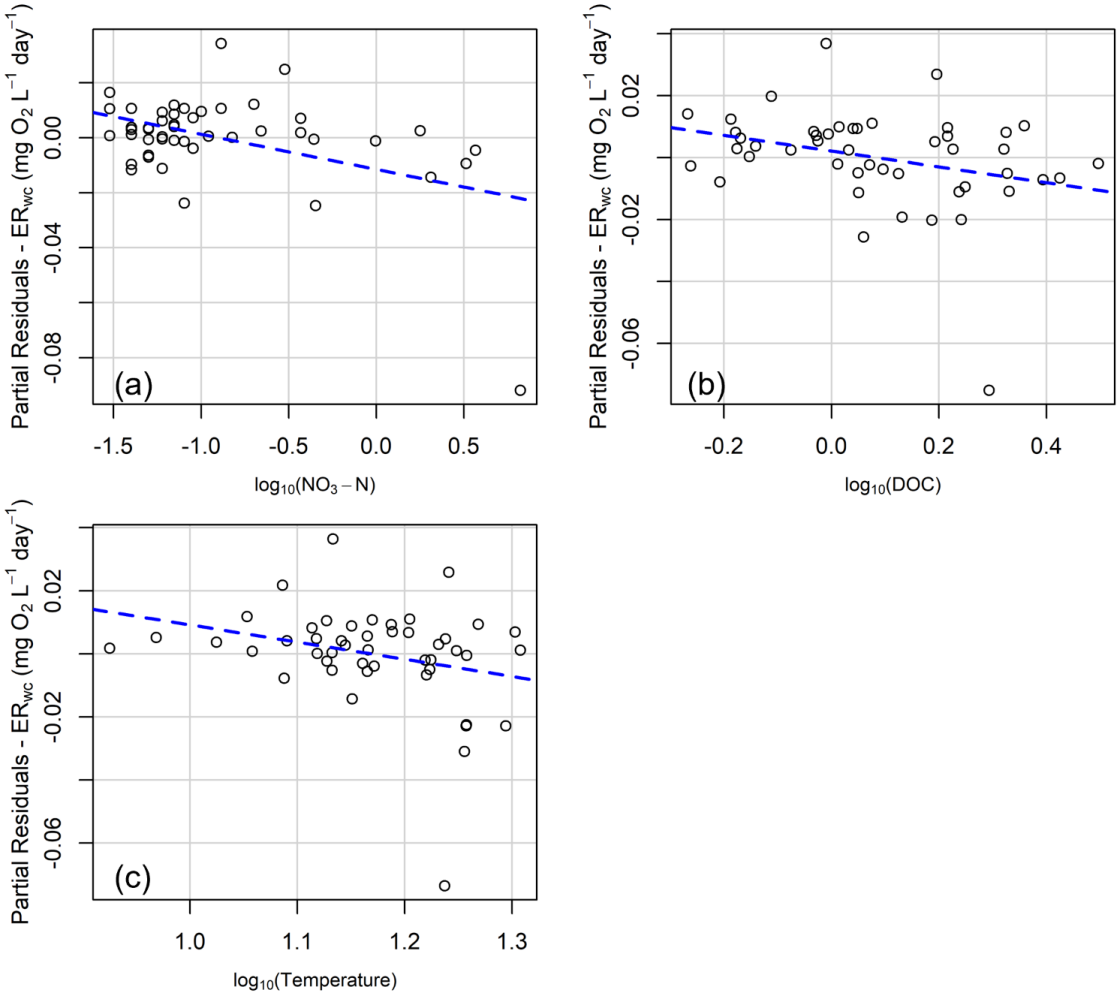

Figure 6. Partial residual plots showing the nature of the relationship between ER_{wc} and explanatory variables retained in the multiple regression model. The best fit model was determined using step-wise forward selection with Akaike Information Criteria adjusted for small sample size (ΔAIC_c) as our model selection criteria. (a) NO_3-N. (b) DOC. (c) Temperature. X-axis variables are reported as the $\log_{10}$ of the mean value for each explanatory variable (NO_3-N, mg L^{-1}; DOC, mg L^{-1}; and water temperature, °C). Y-axis variables are reported as the partial residual variation in ER_{wc} explained by each individual explanatory variable after controlling for the remaining two explanatory variables. Open circles represent individual field sites, and the dashed blue lines are linear regression models fit to the partial residuals.

https://doi.org/10.5194/egusphere-2023-3038
Preprint. Discussion started: 15 January 2024

While ER_{wc} may be a small component of Yakima River basin ER_{tot}, water column processes in the basin may still be relevant to other biogeochemical processes such as the cycling and downstream transport of C and N (Reisinger et al., 2015). In-stream metabolism relies on terrestrially-driven inputs of organic C (OC), which support heterotrophic metabolism that degrades and removes OC input through respiration (Plont et al., 2022; Hall et al., 2016; Allan et al., 2021a). Metabolism can also drive nutrient uptake both at the reach-scale and in the water column specifically (Hall and Tank, 2003; Hall et al., 2009; Reisinger et al., 2015). Nitrogen assimilation into biomass is the primary mechanism for N removal from the water column (Peterson et al., 2001; Mulholland et al., 2008; Hall et al., 2009; Tank et al., 2018), although dissimilatory processes such as nitrification and denitrification also contribute to removal, although denitrification is not likely to contribute to the same extent as denitrification processes that occur in benthic sediments (Peterson et al., 2001; Mulholland et al., 2008). Nitrogen and phosphorus are usually the most limiting nutrients in clear, freshwater rivers such as the Yakima River and its tributaries (Carroll, 2022). Large improvements in water quality draining to the Yakima River and its tributaries from agricultural wastewater drainages ("Wasteways") throughout the Yakima River basin have decreased nutrient and TSS loads to these rivers (Appel et al., 2011). Total dissolved nitrogen (TDN; data not shown, see Grieger et al. (2022)) concentrations throughout the basin (median: 0.19 mg L^{-1}, mean: 0.38 mg L^{-1}) were within reference conditions (i.e., representing the least impacted conditions and intended to be protective of designated uses) set by the U.S. Environmental Protection Agency (EPA) for the lower Yakima River (1.468 mg L^{-1}; Yakima River at Mabton); however, TDN concentrations exceeded reference conditions for the Naches River (0.166 mg L^{-1}), a major tributary to the Yakima River (Wise et al., 2009). Similarly, NO_3-N concentrations (median: 0.07 mg L^{-1}, mean: 0.51 mg L^{-1}) were within reference conditions for nitrite+nitrate for the lower Yakima River (1.095 mg L^{-1}; Yakima River at Mabton) but exceeded reference conditions for nitrite+nitrate for the Naches River (0.031 mg L^{-1}).

Our results also have implications for C cycling across stream networks. We observed faster ER_{wc} with higher values of DOC. The positive relationships between ER_{wc} and NO_3-N, DOC, and temperature all make conceptual sense in that faster respiration will occur when there are more nutrients and DOC available at higher temperatures. The generally low TSS concentrations observed during our study period may inhibit ER_{wc} in rivers throughout the basin. Suspended sediment can control ER_{wc} (Honious et al., 2021). We suspect that high suspended sediment loads in turbid Midwestern and western rivers (Reisinger et al. (2021) and rivers in the Amazon River basin (Ellis et al., 2012) may be one of the primary factors controlling water column respiration rates. TSS loads stimulate the processing of OM in the water column (Gardner and Doyle, 2018). One major difference between the Yakima River basin and the Amazon River basin is relatively low TSS during our study period. Low TSS is potentially causing the very slow ER_{wc} rates throughout the Yakima basin. The formation of bacterial assemblages (i.e., bacterioplankton) on suspended sediment contribute substantially to material processing in the water column, particularly in larger rivers starting around 5th order and higher (Millar et al., 2015; Ochs et al., 2013; Reisinger et al., 2015). The increased surface area of suspended particles in the water column provides microsite habitats for microorganisms (Ochs et al., 2010; Liu et al., 2013). It is likely that most bacterial production and enzymatic activity occur on suspended sediments (Gardner and Doyle, 2018). Using a model based on geomorphic and hydrologic principles to estimate the total surface area of individual sediment particles in contact with surface water in the water column and benthic zone (R_{SA}), they found more sediment-water contact area in the water column than in the benthic zone and that the ratio of water column to benthic sediment contact area scaled as a power function of watershed area (Gardner and Doyle, 2018).

https://doi.org/10.5194/egusphere-2023-3038
Preprint. Discussion started: 15 January 2024

4 Conclusions, limitations, and next steps

Here we established that the very slow rates of water column respiration observed in rivers and streams across the Yakima River basin were 10–30× smaller than published rates from similar studies conducted in temperate and tropical rivers across the CONUS and in the Amazon River basin, respectively. We also concluded that ER_{wc} did not likely contribute much to ER_{tot} throughout the basin. Our model results showed that variation in ER_{wc} is well explained by NO_3-N, DOC, and stream temperature and found that ER_{wc} rates in Yakima River basin rivers and streams increase linearly with increasing NO_3-N, DOC, and stream temperature. In addition to low temperatures and low concentrations of NO_3-N and DOC, we also observed low TSS concentrations during our sampling period and we infer that it is likely all four of these factors that combined to cause extremely slow ER_{wc} throughout the Yakima River basin.

A practical implication of very slow ER_{wc} is that estimating ER_{tot} (e.g., via *in situ* DO sensors)—which integrates contributions from water column respiration and sediment-associated respiration (ER_{sed}), including respiration from biofilms and hyporheic zone processes (Plont et al., 2022)—in rivers like those in the Yakima River basin will essentially measure ER_{sed}. Isolating respiration from the sediment/benthic portion of river systems is challenging and is often done via localized incubation bottle measurements that do not provide integrated reach-scale rates. The Yakima River basin and other basins with very slow ER_{wc} provide an opportunity to study spatiotemporal variation in reach-scale ER_{sed} via *in situ* DO sensors. Cold, clear rivers such as those in the Yakima River basin can be useful in parsing ER_{wc} and ER_{sed} contributions to ER_{tot} in future metabolism studies because ER_{sed} is often, though not always, the dominant component of respiration in river systems. The slow rates of ER_{wc} across the Yakima River basin support modeling work on ecosystem metabolism across the basin and the broader Columbia River basin that focused on reactions occurring within and below the riverbed (Son et al., 2022). Those modeling efforts provide predictions of ER_{sed} spatial variation that remain untested. We propose that stream metabolism, at least during baseflow conditions, across the basin is due almost entirely to activity along, within, and below the streambed simply because ER_{wc} was so slow. Mechanistic understanding of spatiotemporal variation in ER_{tot} throughout the Yakima River basin is, therefore, likely to come from knowledge of riverbed-associated respiration. Except for much larger, deeper rivers like the mainstem Columbia River, where water column processes dominate (Roley et al., 2023; Ellis et al., 2012; Caraco and Cole, 1999), this inference is likely to hold true across much of the broader Columbia River basin as our field sites spanned locations that represented biophysical and hydrologic characteristics across the Columbia River basin (Table 1). We encourage taking advantage of rivers with slow ER_{wc} to test process model predictions by studying ER_{sed} via *in situ* sensors. Such a test can provide *in situ* rate estimates that align with the spatial scale of model predictions, whereby both measurements and models are operating at the reach-scale (e.g., 10s to 100s of meters).

Future work will expand our current Yakima River basin river metabolism study by collecting both ER_{wc} and ER_{tot} measurements throughout the basin to estimate ER_{sed}. To overcome potential limitations of our current study as well as investigate the primary drivers of spatial variability in ER_{sed}, we will be evaluating the effect of a broader range of environmental conditions, including fluvial geomorphic characteristics, on respiration rates throughout the basin. We also hope to include a broader range of stream orders; this study included orders 2–7, with order 7 being the highest order in the Yakima River basin. Aquatic material processing can shift between 5th and 9th order rivers, from occurring primarily in benthic sediments to occurring primarily in the water column (Gardner and Doyle, 2018; Reisinger et al., 2021). For example, production of nitrous oxide (N_2O) in the water column increased with river size (Marzadri et al., 2021). Similarly, ammonium (NH_4) production increased with increasing river size, while denitrification in the water column dominated in mid-sized rivers (Reisinger, 2015; Reisinger et al., 2016). Because large rivers carry loads of suspended sediment and have the potential to support planktonic communities, water column material processing

https://doi.org/10.5194/egusphere-2023-3038
Preprint. Discussion started: 15 January 2024

may only be important in the largest rivers (Gardner and Doyle, 2018; Reynolds and Descy, 1996). However, a recent study by Roley et al. (2023) on reach-scale metabolism in the mainstem Columbia River found ER_{tot} rates similar in scale to ER_{wc} rates measured by Reisinger et al. (2021) in mid-sized turbid midwestern and clear and turbid western rivers. Despite these limitations and future research needs, the Yakima River basin is representative of the vast majority of the broader Columbia River basin (excluding the Columbia River itself) and we propose that at least during baseflow conditions, nearly all ER_{tot} will be from ER_{sed}, with small contributions from ER_{wc}. This small contribution is most likely due to low turbidity, low nutrient concentrations, and low temperatures in the water column.

Code and data availability

The minimal data set and statistical analysis code ("data package") underlying the findings in our study will be published at the U.S. Department of Energy's Environmental System Science Data Infrastructure for a Virtual Ecosystem (ESS-DIVE) repository (https://ess-dive.lbl.gov/about/) prior to publication. Following internal review, the authors will submit the data package to ESS-DIVE for approval and, upon approval, a persistent DOI will be assigned to data package. The full data sets (i.e., sensor data; surface water chemistry data; and geospatial information, metadata, and maps for 2021 Spatial Study sampling event) and statistical analysis code from which the minimal data set was acquired can be accessed at the ESS-DIVE repository, including 1) "Spatial Study 2021: Sensor-Based Time Series of Surface Water Temperature, Specific Conductance, Total Dissolved Solids, Turbidity, pH, and Dissolved Oxygen from across Multiple Watersheds in the Yakima River Basin, Washington, USA (v2)" (Fulton et al., 2022) (https://data.ess-dive.lbl.gov/view/doi:10.15485/1892052); 2) "Spatial Study 2021: Sample-Based Surface Water Chemistry and Organic Matter Characterization across Watersheds in the Yakima River Basin, Washington, USA (v2)" (Grieger et al., 2022) (https://data.ess-dive.lbl.gov/view/doi:10.15485/1898914); and 3) "Geospatial Information, Metadata, and Maps for Global River Corridor Science Focus Area Sites (v2)" (Kaufman et al., 2023) (https://data.ess-dive.lbl.gov/datasets/doi:10.15485/1971251).

Supplement link

The persistent DOI and the link to the Supplementary Material will be supplied by EGU Biogeosciences prior to publication.

Author contributions

Conceptualization: JCS, MHK, ROH, SGF
Data Curation: SGF, YF, BF, VGC, AEG, SG, MHK, XL, AM, OO, and KS
Formal Analysis: SGF, VGC, MHK, XL, AM, OO, and JT
Funding Acquisition: XC, TDS, and JCS
Investigation: SGF, MB, MAB, VGC, SG, MHK, XL, SAM, AM, OO, AP, HR, LR, KS, JT, KS, JMT, and JCS
Methodology: SGF, MHK, VGC, ROH, XL, SAM, AM, OO, HR, LR, KS, JT, and JCS
Project Administration: SGF, VGC, SG, MHK, SAM, AM, OO, LR, and JCS
Resources: SGF, VGC, SG, MHK, SAM, AM, OO, and LR
Software: SGF, VGC, BF, MHK, XL, AM, KS, and EM
Supervision: XC, MHK, TDS, and JCS
Validation: SGF, VGC, SG, MHK, XL, AM, OO, HR, and JCS
Visualization: BF, SGF, MHK, XL, SAM, and JT

https://doi.org/10.5194/egusphere-2023-3038
Preprint. Discussion started: 15 January 2024

Writing – Original Draft Preparation: SGF, VGC, MHK, AM, JT, and JCS
Writing – Review & Editing: SGF, MB, VGC, BF, AEG, ROH, MHK, AM, KS, JT, and JCS

Competing interest

The authors declare that they have no conflict of interest.

Acknowledgements

This research was supported by the U.S. Department of Energy (DOE), Office of Science, Office of Biological and Environmental Research, Environmental System Science (ESS) Program (https://ess.science.energy.gov/). This contribution originates from the River Corridor Scientific Focus Area (SFA) project at Pacific Northwest National Laboratory (PNNL). PNNL is operated by Battelle Memorial Institute for the U.S. DOE under Contract No. DE-AC05-76RL01830. FTICR-MS data was generated at the DOE BER Environmental Molecular Science Laboratory User Facility (EMSL; https://www.pnnl.gov/environmental-molecular-sciences-laboratory) under user proposal 60221. Data were collected from the greater Yakima River Basin, located within the homelands of many of the Columbia Plateau tribes. We thank the Confederated Tribes and Bands of the Yakama Nation Tribal Council and Yakama Nation Fisheries for working with us to facilitate sample collection and optimization of data usage according to their values and worldview. We also thank the US Forest Service (USFS), Washington Department of Natural Resources (WDNR), and Washington Department of Fish and Wildlife (WDFW) for access to field locations where these samples were collected. The authors would also like to thank A.J. Reisinger for providing water column respiration data included in this study for 13 mid-sized turbid midwestern rivers and western rivers (Reisinger et al., 2021) as well as helpful insights and discussions with the lead author on the state-of-the-science on water column respiration.

References

The National Map Download (v2.0): https://apps.nationalmap.gov/downloader/, last access: June 29, 2023.

PRISM Climate Group: http://www.prismclimate.org, last access: June 29, 2023.

Ahmed, S. and Abdul-Aziz, O. I.: Metabolic scaling of stream dissolved oxygen across the U.S. Atlantic Coast, Science of The Total Environment, 821, 153292, 10.1016/j.scitotenv.2022.153292, 2022.

Aho, K., Derryberry, D., and Peterson, T.: Model selection for ecologists: the worldviews of AIC and BIC, Ecology, 95, 631-636, https://doi.org/10.1890/13-1452.1, 2014.

Alexander, R. B., Smith, R. A., and Schwarz, G. E.: Effect of stream channel size on the delivery of nitrogen to the Gulf of Mexico, Nature, 403, 758-761, 10.1038/35001562, 2000.

Alexander, R. B., Boyer, E. W., Smith, R. A., Schwarz, G. E., and Moore, R. B.: The Role of Headwater Streams in Downstream Water Quality, Journal of the American Water Resources Association, 43, 41-59, 10.1111/j.1752-1688.2007.00005.x, 2007.

Allan, J. D., Castillo, M. M., and Capps, K. A.: Carbon Dynamics and Stream Ecosystem Metabolism, in: Stream Ecology : Structure and Function of Running Waters, Springer International Publishing, Cham, 421-452, 10.1007/978-3-030-61286-3_14, 2021a.

Allan, J. D., Castillo, M. M., and Capps, K. A.: Carbon Dynamics and Stream Ecosystem Metabolism, in, Springer International Publishing, 421-452, 10.1007/978-3-030-61286-3_14, 2021b.

https://doi.org/10.5194/egusphere-2023-3038
Preprint. Discussion started: 15 January 2024

Alnoee, A. B., Levi, P. S., Baattrup-Pedersen, A., and Riis, T.: Macrophytes enhance reach-scale metabolism on a daily, seasonal and annual basis in agricultural lowland streams, Aquatic Sciences, 83, http://dx.doi.org/10.1007/s00027-020-00766-4, 2021.

Appel, M., Little, R., Wendt, H., and Nielson, M.: Assessment of the Lower Yakima River in Benton County, Washington, Benton Conservation District, 182, 2011.

Appling, A. P., Hall, R. O., Yackulic, C. B., and Arroita, M.: Overcoming Equifinality: Leveraging Long Time Series for Stream Metabolism Estimation, Journal of Geophysical Research: Biogeosciences, 123, 624-645, 10.1002/2017jg004140, 2018a.

Appling, A. P., Read, J. S., Winslow, L. A., Arroita, M., Bernhardt, E. S., Griffiths, N. A., Hall, R. O., Jr., Harvey, J. W., Heffernan, J. B., Stanley, E. H., Stets, E. G., and Yackulic, C. B.: The metabolic regimes of 356 rivers in the United States, Scientific Data, 5, 180292, 10.1038/sdata.2018.292, 2018b.

Appling, A. P., Read, J. S., Winslow, L. A., Arroita, M., Bernhardt, E. S., Griffiths, N. A., Hall, R. O., Jr., Harvey, J. W., Heffernan, J. B., Stanley, E. H., Stets, E. G., and Yackulic, C. B.: Metabolism estimates for 356 U.S. rivers (2007-2017): U.S. Geological Survey data release [dataset], https://doi.org/10.5066/F70864KX, 2018c.

Bates, D., Mächler, M., Bolker, B., and Walker, S.: Fitting Linear Mixed-Effects Models Using lme4, Journal of Statistical Software, 67, 1 - 48, 10.18637/jss.v067.i01, 2015.

Battin, T. J., Kaplan, L. A., Findlay, S., Hopkinson, C. S., Marti, E., Packman, A. I., Newbold, J. D., and Sabater, F.: Biophysical controls on organic carbon fluxes in fluvial networks, Nature Geoscience, 1, 95-100, 10.1038/ngeo101, 2008.

Bernhardt, E. S., Heffernan, J. B., Grimm, N. B., Stanley, E. H., Harvey, J. W., Arroita, M., Appling, A. P., Cohen, M. J., McDowell, W. H., Hall, R. O., Read, J. S., Roberts, B. J., Stets, E. G., and Yackulic, C. B.: The metabolic regimes of flowing waters, Limnology and Oceanography, 63, S99-S118, 10.1002/lno.10726, 2018.

Bernhardt, E. S., Savoy, P., Vlah, M. J., Appling, A. P., Koenig, L. E., Hall, R. O., Arroita, M., Blaszczak, J. R., Carter, A. M., Cohen, M., Harvey, J. W., Heffernan, J. B., Helton, A. M., Hosen, J. D., Kirk, L., McDowell, W. H., Stanley, E. H., Yackulic, C. B., and Grimm, N. B.: Light and flow regimes regulate the metabolism of rivers, Proceedings of the National Academy of Sciences, 119, e2121976119, 10.1073/pnas.2121976119, 2022.

Bernot, M. J., Sobota, D. J., Hall, R. O., Mulholland, P. J., Dodds, W. K., Webster, J. R., Tank, J. L., Ashkenas, L. R., Cooper, L. W., Dahm, C. N., Gregory, S. V., Grimm, N. B., Hamilton, S. K., Johnson, S. L., McDowell, W. H., Meyer, J. L., Peterson, B., Poole, G. C., Valett, H. M., Arango, C., Beaulieu, J. J., Burgin, A. J., Crenshaw, C., Helton, A. M., Johnson, L., Merriam, J., Niederlehner, B. R., O'Brien, J. M., Potter, J. D., Sheibley, R. W., Thomas, S. M., and Wilson, K.: Inter-regional comparison of land-use effects on stream metabolism, Freshwater Biology, 55, 1874-1890, 10.1111/j.1365-2427.2010.02422.x, 2010.

Bertuzzo, E., Hotchkiss, E. R., Argerich, A., Kominoski, J. S., Oviedo-Vargas, D., Savoy, P., Scarlett, R., Von Schiller, D., and Heffernan, J. B.: Respiration regimes in rivers: Partitioning source-specific respiration from metabolism time series, Limnology and Oceanography, 10.1002/lno.12207, 2022.

Bórquez-López, R. A., Martínez-Córdova, L. R., Gil-Nuñez, J. C., González-Galaviz, J. R., Ibarra Gámez, J. C., and Casillas-Hernández, R.: Implementation and Evaluation of Open-Source Hardware to Monitor Water Quality in Precision Aquaculture, Sensors, 20, 6112, 2020.

Bramer, L. M., White, A. M., Stratton, K. G., Thompson, A. M., Claborne, D., Hofmockel, K., and McCue, L. A.: ftmsRanalysis: An R package for exploratory data analysis and interactive visualization of FT-MS data, PLOS Computational Biology, 16, e1007654, 10.1371/journal.pcbi.1007654, 2020.

Burnham, K. P. and Anderson, D. R., Burnham, K. P., and Anderson, D. R. (Eds.): Model Selection and Multimodel Inference: A Practical Information-Theoretic Approach, 2, Springer, New York, NY, 488 pp., https://doi.org/10.1007/b97636, 2007.

https://doi.org/10.5194/egusphere-2023-3038
Preprint. Discussion started: 15 January 2024

Caraco, N. F. and Cole, J. J.: Regional scale export of C, N, P and sediment: What river data tell us about key controlling variables, in: Integrating hydrology, ecosystem dynamics, and biogeochemistry in complex landscapes, edited by: Tenhunen, J. D., and Kabat, P., Wiley, New York, NY, 239–253, 1999.

Carlson, S. P. and Poole, G. C.: Influences of stream ecosystem respiration on stream network denitrification: Results from a simulation modeling experiment, Freshwater Science, 41, 363-375, 10.1086/720720, 2022.

Carroll, J.: Quality Assurance Project Plan: Lower Yakima River Monitoring for Aquatic Life Parameters to Support Water Quality Gaging., Washington State Department of Ecology, Olympia, WA, 40, 2022.

Clapcott, J. E. and Barmuta, L. A.: Metabolic patch dynamics in small headwater streams: exploring spatial and temporal variability in benthic processes, Freshwater Biology, 55, 806-824, 10.1111/j.1365-2427.2009.02324.x, 2010.

Cory, R. M., Ward, C. P., Crump, B. C., and Kling, G. W.: Sunlight controls water column processing of carbon in arctic fresh waters, Science, 345, 925-928, doi:10.1126/science.1253119, 2014.

del Giorgio, P. A. and Williams, P. J. l. B.: Respiration in Aquatic Ecosystems, Oxford University Press, Oxford, United Kingdom, 315 pp.2005.

Demars, B. O. L.: Hydrological pulses and burning of dissolved organic carbon by stream respiration, Limnology and Oceanography, 64, 406-421, 10.1002/lno.11048, 2019.

Devol, A. H., Forsberg, B. R., Richey, J. E., and Pimentel, T. P.: Seasonal variation in chemical distributions in the Amazon (Solimões) River: A multiyear time series, Global Biogeochemical Cycles, 9, 307-328, https://doi.org/10.1029/95GB01145, 1995.

Diamond, J. S., Moatar, F., Cohen, M. J., Poirel, A., Martinet, C., Maire, A., and Pinay, G.: Metabolic regime shifts and ecosystem state changes are decoupled in a large river, Limnology and Oceanography, 10.1002/lno.11789, 2021a.

Diamond, J. S., Bernal, S., Boukra, A., Cohen, M. J., Lewis, D., Masson, M., Moatar, F., and Pinay, G.: Stream network variation in dissolved oxygen: Metabolism proxies and biogeochemical controls, Ecological Indicators, 131, 108233, 10.1016/j.ecolind.2021.108233, 2021b.

Dillon, G. K.: Wildfire Hazard Potential (WHP) for the conterminous United States (270-m GRID), version 2018 continuous (2nd Edition), Forest Service Research Data Archive [dataset], https://doi.org/10.2737/RDS-2015-0047-2, 2018.

Dillon, G. K. and Gilbertson-Day, J. W.: Wildfire Hazard Potential for the United States (270-m), version 2020, https://doi.org/10.2737/RDS-2015-0047-3, 2020.

Dittmar, T., Koch, B., Hertkorn, N., and Kattner, G.: A simple and efficient method for the solid-phase extraction of dissolved organic matter (SPE-DOM) from seawater, Limnology and Oceanography: Methods, 6, 230-235, 10.4319/lom.2008.6.230, 2008.

Ellis, E. E., Richey, J. E., Aufdenkampe, A. K., Krusche, A. V., Quay, P. D., Salimon, C., and Da Cunha, H. B.: Factors controlling water-column respiration in rivers of the central and southwestern Amazon Basin, Limnology and Oceanography, 57, 527-540, 10.4319/lo.2012.57.2.0527, 2012.

Findlay, S.: Importance of surface-subsurface exchange in stream ecosystems: The hyporheic zone, Limnology and Oceanography, 40, 159-164, 10.4319/lo.1995.40.1.0159, 1995.

Finlay, J. C.: Stream size and human influences on ecosystem production in river networks, Ecosphere, 2, art87, 10.1890/es11-00071.1, 2011.

Friedl, M. and Sulla-Menashe, D.: MCD12Q1 MODIS/Terra+Aqua Land Cover Type Yearly L3 Global 500m SIN Grid V006 [dataset], 10.5067/MODIS/MCD12Q1.006, 2019.

Fulton, S. G., Barnes, M., Borton, M. A., Chen, X., Farris, Y., Forbes, B., Garayburu-Caruso, V. A., Goldman, A. E., Grieger, S., Kaufman, M. H., Lin, X., McKever, S. A., Myers-Pigg, A., Otenburg, O., Pelly, A., Ren, H., Renteria, L., Scheibe, T. D., Son, K., Torgeson, J. M., and Stegen, J. C.: Spatial Study 2021: Sensor-Based Time Series of Surface Water Temperature, Specific

https://doi.org/10.5194/egusphere-2023-3038
Preprint. Discussion started: 15 January 2024

Conductance, Total Dissolved Solids, Turbidity, pH, and Dissolved Oxygen from across Multiple Watersheds in the Yakima River Basin, Washington, USA (v2) [dataset], 10.15485/1892052, 2022.

Gagne-Maynard, W. C., Ward, N. D., Keil, R. G., Sawakuchi, H. O., Da Cunha, A. C., Neu, V., Brito, D. C., Da Silva Less, D. F., Diniz, J. E. M., De Matos Valerio, A., Kampel, M., Krusche, A. V., and Richey, J. E.: Evaluation of Primary Production in the Lower Amazon River Based on a Dissolved Oxygen Stable Isotopic Mass Balance, Frontiers in Marine Science, 4, 10.3389/fmars.2017.00026, 2017.

Garayburu-Caruso, V. A., Stegen, J. C., Song, H.-S., Renteria, L., Wells, J., Garcia, W., Resch, C. T., Goldman, A. E., Chu, R. K., Toyoda, J., and Graham, E. B.: Carbon Limitation Leads to Thermodynamic Regulation of Aerobic Metabolism, Environmental Science & Technology Letters, 7, 517-524, 10.1021/acs.estlett.0c00258, 2020a.

Garayburu-Caruso, V. A., Danczak, R. E., Stegen, J. C., Renteria, L., McCall, M., Goldman, A. E., Chu, R. K., Toyoda, J., Resch, C. T., Torgeson, J. M., Wells, J., Fansler, S., Kumar, S., and Graham, E. B.: Using Community Science to Reveal the Global Chemogeography of River Metabolomes, Metabolites, 10, 518, 10.3390/metabo10120518, 2020b.

Gardner, J. R. and Doyle, M. W.: Sediment–Water Surface Area Along Rivers: Water Column Versus Benthic, Ecosystems, 21, 1505-1520, 10.1007/s10021-018-0236-2, 2018.

Genzoli, L. and Hall, R. O., Jr: Shifts in Klamath River metabolism following a reservoir cyanobacterial bloom, Freshwater Science, 35, 795-809, 10.1086/687752, 2016.

Gomez-Velez, J. D., Harvey, J. W., Cardenas, M. B., and Kiel, B.: Denitrification in the Mississippi River network controlled by flow through river bedforms, Nature Geoscience, 8, 941-945, 10.1038/ngeo2567, 2015.

Grieger, S., Barnes, M., Borton, M. A., Chen, X., Chu, R., Farris, Y., Forbes, B., Fulton, S. G., Garayburu-Caruso, V. A., Goldman, A. E., Gonzalez, B. I., Kaufman, M. H., McKever, S. A., Myers-Pigg, A., Otenburg, O., Pelly, A., Renteria, L., Scheibe, T. D., Son, K., Torgeson, J. M., Toyoda, J. G., and Stegen, J. C.: Spatial Study 2021: Sample-Based Surface Water Chemistry and Organic Matter Characterization across Watersheds in the Yakima River Basin, Washington, USA (v2) [dataset], 10.15485/1898914, 2022.

Grimm, N. B. and Fisher, S. G.: Exchange between interstitial and surface water: Implications for stream metabolism and nutrient cycling, Hydrobiologia, 111, 219-228, 10.1007/BF00007202, 1984.

Gu, S., Li, S., and Santos, I. R.: Anthropogenic land use substantially increases riverine CO2 emissions, Journal of Environmental Sciences, 118, 158-170, https://doi.org/10.1016/j.jes.2021.12.040, 2022.

Hall, R. O. and Hotchkiss, E. R.: Chapter 34 - Stream Metabolism, in: Methods in Stream Ecology (Third Edition), edited by: Lamberti, G. A., and Hauer, F. R., Academic Press, 219-233, https://doi.org/10.1016/B978-0-12-813047-6.00012-7, 2017.

Hall, R. O., Tank, J. L., Baker, M. A., Rosi-Marshall, E. J., and Hotchkiss, E. R.: Metabolism, Gas Exchange, and Carbon Spiraling in Rivers, Ecosystems, 19, 73-86, 10.1007/s10021-015-9918-1, 2016.

Hall, R. O., Tank, J. L., Sobota, D. J., Mulholland, P. J., O'Brien, J. M., Dodds, W. K., Webster, J. R., Valett, H. M., Poole, G. C., Peterson, B. J., Meyer, J. L., McDowell, W. H., Johnson, S. L., Hamilton, S. K., Grimm, N. B., Gregory, S. V., Dahm, C. N., Cooper, L. W., Ashkenas, L. R., Thomas, S. M., Sheibley, R. W., Potter, J. D., Niederlehner, B. R., Johnson, L. T., Helton, A. M., Crenshaw, C. M., Burgin, A. J., Bernot, M. J., Beaulieu, J. J., and Arangob, C. P.: Nitrate removal in stream ecosystems measured by 15N addition experiments: Total uptake, Limnology and Oceanography, 54, 653-665, 10.4319/lo.2009.54.3.0653, 2009.

Hall, R. O., Jr. and Tank, J. L.: Ecosystem metabolism controls nitrogen uptake in streams in Grand Teton National Park, Wyoming, Limnology and Oceanography, 48, 1120-1128, 10.4319/lo.2003.48.3.1120, 2003.

Hensley, R. T., Kirk, L., Spangler, M., Gooseff, M. N., and Cohen, M. J.: Flow Extremes as Spatiotemporal Control Points on River Solute Fluxes and Metabolism, Journal of Geophysical Research: Biogeosciences, 124, 537-555, 10.1029/2018jg004738, 2019.

https://doi.org/10.5194/egusphere-2023-3038
Preprint. Discussion started: 15 January 2024

Hoellein, T. J., Bruesewitz, D. A., and Richardson, D. C.: Revisiting Odum (1956): A synthesis of aquatic ecosystem metabolism, Limnology and Oceanography, 58, 2089-2100, 10.4319/lo.2013.58.6.2089, 2013.

Hoellein, T. J., Tank, J. L., Rosi-Marshall, E. J., Entrekin, S. A., and Lamberti, G. A.: Controls on spatial and temporal variation of nutrient uptake in three Michigan headwater streams, Limnology and Oceanography, 52, 1964-1977, 10.4319/lo.2007.52.5.1964, 2007.

Honious, S. A. S., Hale, R. L., Guilinger, J. J., Crosby, B. T., and Baxter, C. V.: Turbidity Structures the Controls of Ecosystem Metabolism and Associated Metabolic Process Domains Along a 75-km Segment of a Semiarid Stream, Ecosystems, 10.1007/s10021-021-00661-5, 2021.

Hornbach, D. J.: Multi-Year Monitoring of Ecosystem Metabolism in Two Branches of a Cold-Water Stream, Environments, 8, 19, 2021.

Hotchkiss, E. R. and Hall, R. O., Jr.: High rates of daytime respiration in three streams: Use of δ 18 OO2 and O2 to model diel ecosystem metabolism, Limnology and Oceanography, 59, 798-810, 10.4319/lo.2014.59.3.0798, 2014.

Hotchkiss, E. R., Hall Jr, R. O., Sponseller, R. A., Butman, D., Klaminder, J., Laudon, H., Rosvall, M., and Karlsson, J.: Sources of and processes controlling CO2 emissions change with the size of streams and rivers, Nature Geoscience, 8, 696-699, 10.1038/ngeo2507, 2015.

Isabel, P., Kuglerová, L., García, L., and Martí, E.: Nutrient availability modulates the effect of water abstraction on the metabolism of 2 lowland forested streams, Freshwater Science, 10.1086/719990, 2022.

Jankowski, K. J. and Schindler, D. E.: Watershed geomorphology modifies the sensitivity of aquatic ecosystem metabolism to temperature, Sci Rep, 9, 17619, 10.1038/s41598-019-53703-3, 2019.

Kaufman, M. H., Barnes, M., Chen, X., Forbes, B., Garayburu-Caruso, V. A., Goldman, A. E., Stegen, J. C., Myers-Pigg, A., and Scheibe, T. D.: Geospatial Information, Metadata, and Maps for Global River Corridor Science Focus Area Sites (v2) [dataset], 10.15485/1971251, 2023.

Kirk, L., Hensley, R. T., Savoy, P., Heffernan, J. B., and Cohen, M. J.: Estimating Benthic Light Regimes Improves Predictions of Primary Production and constrains Light-Use Efficiency in Streams and Rivers, Ecosystems, 24, 825-839, 10.1007/s10021-020-00552-1, 2021.

Koenig, L. E., Helton, A. M., Savoy, P., Bertuzzo, E., Heffernan, J. B., Hall Jr., R. O., and Bernhardt, E. S.: Emergent productivity regimes of river networks, Limnology and Oceanography Letters, 4, 173-181, https://doi.org/10.1002/lol2.10115, 2019.

Liu, T., Xia, X., Liu, S., Mou, X., and Qiu, Y.: Acceleration of Denitrification in Turbid Rivers Due to Denitrification Occurring on Suspended Sediment in Oxic Waters, Environmental Science & Technology, 47, 4053-4061, 10.1021/es304504m, 2013.

Marzadri, A., Dee, M. M., Tonina, D., Bellin, A., and Tank, J. L.: Role of surface and subsurface processes in scaling N2O emissions along riverine networks, Proceedings of the National Academy of Sciences, 114, 4330-4335, 10.1073/pnas.1617454114, 2017.

Marzadri, A., Amatulli, G., Tonina, D., Bellin, A., Shen, L. Q., Allen, G. H., and Raymond, P. A.: Global riverine nitrous oxide emissions: The role of small streams and large rivers, Science of The Total Environment, 776, 145148, 10.1016/j.scitotenv.2021.145148, 2021.

McKay, L., Bondelid, T., Dewald, T., Johnston, J., Moore, R., and Rea, A.: NHDPlus Version 2: User Guide, 2012.

Mejia, F. H., Fremier, A. K., Benjamin, J. R., Bellmore, J. R., Grimm, A. Z., Watson, G. A., and Newsom, M.: Stream metabolism increases with drainage area and peaks asynchronously across a stream network, Aquatic Sciences, 81, 10.1007/s00027-018-0606-z, 2019.

https://doi.org/10.5194/egusphere-2023-3038
Preprint. Discussion started: 15 January 2024

Millar, J. J., Payne, J. T., Ochs, C. A., and Jackson, C. R.: Particle-associated and cell-free extracellular enzyme activity in relation to nutrient status of large tributaries of the Lower Mississippi River, Biogeochemistry, 124, 255-271, 10.1007/s10533-015-0096-1, 2015.

Mulholland, P. J., Fellows, C. S., Tank, J. L., Grimm, N. B., Webster, J. R., Hamilton, S. K., Martí, E., Ashkenas, L., Bowden, W. B., Dodds, W. K., McDowell, W. H., Paul, M. J., and Peterson, B. J.: Inter-biome comparison of factors controlling stream metabolism, Freshwater Biology, 46, 1503-1517, 10.1046/j.1365-2427.2001.00773.x, 2001.

Mulholland, P. J., Helton, A. M., Poole, G. C., Hall, R. O., Hamilton, S. K., Peterson, B. J., Tank, J. L., Ashkenas, L. R., Cooper, L. W., Dahm, C. N., Dodds, W. K., Findlay, S. E. G., Gregory, S. V., Grimm, N. B., Johnson, S. L., McDowell, W. H., Meyer, J. L., Valett, H. M., Webster, J. R., Arango, C. P., Beaulieu, J. J., Bernot, M. J., Burgin, A. J., Crenshaw, C. L., Johnson, L. T., Niederlehner, B. R., O'Brien, J. M., Potter, J. D., Sheibley, R. W., Sobota, D. J., and Thomas, S. M.: Stream denitrification across biomes and its response to anthropogenic nitrate loading, Nature, 452, 202-205, 10.1038/nature06686, 2008.

Myneni, R., Knyazikhin, Y., and Park, T.: MCD15A3H MODIS/Terra+Aqua Leaf Area Index/FPAR 4-day L4 Global 500m SIN Grid V006. [dataset], https://doi.org/10.5067/MODIS/MCD15A3H.006, 2015.

Naegeli, M. W. and Uehlinger, U.: Contribution of the Hyporheic Zone to Ecosystem Metabolism in a Prealpine Gravel-Bed-River, Journal of the North American Benthological Society, 16, 794-804, 10.2307/1468172, 1997.

Nakano, D., Iwata, T., Suzuki, J., Okada, T., Yamamoto, R., and Imamura, M.: The effects of temperature and light on ecosystem metabolism in a Japanese stream, Freshwater Science, 41, 113-124, 10.1086/718648, 2022.

Ochs, C. A., Capello, H. E., and Pongruktham, O.: Bacterial production in the Lower Mississippi River: importance of suspended sediment and phytoplankton biomass, Hydrobiologia, 637, 19-31, 10.1007/s10750-009-9981-8, 2010.

Ochs, C. A., Pongruktham, O., and Zimba, P. V.: Darkness at the break of noon: Phytoplankton production in the Lower Mississippi River, Limnology and Oceanography, 58, 555-568, 10.4319/lo.2013.58.2.0555, 2013.

Peterson, B. J., Wollheim, W. M., Mulholland, P. J., Webster, J. R., Meyer, J. L., Tank, J. L., Martí, E., Bowden, W. B., Valett, H. M., Hershey, A. E., McDowell, W. H., Dodds, W. K., Hamilton, S. K., Gregory, S., and Morrall, D. D.: Control of Nitrogen Export from Watersheds by Headwater Streams, Science, 292, 86-90, doi:10.1126/science.1056874, 2001.

Plont, S., Riney, J., and Hotchkiss, E. R.: Integrating Perspectives on Dissolved Organic Carbon Removal and Whole-Stream Metabolism, J Geophys Res-Biogeo, 127, 10.1029/2021JG006610, 2022.

Quay, P. D., Wilbur, D., Richey, J. E., Devol, A. H., Benner, R., and Forsberg, B. R.: The 18O:16O of dissolved oxygen in rivers and lakes in the Amazon Basin: Determining the ratio of respiration to photosynthesis rates in freshwaters, Limnology and Oceanography, 40, 718-729, 10.4319/lo.1995.40.4.0718, 1995.

R Core Team: R: A language and environment for statistical computing, R Foundation for Statistical Computing [code], 2022.

Reisinger, A. J.: Assessing the Role of the Water Column in Nutrient Dynamics of Lotic Ecosystems, Biological Sciences, University of Notre Dame, Notre Dame, IN, 254 pp., 10.7274/4t64gm82d82, 2015.

Reisinger, A. J., Tank, J. L., Hoellein, T. J., and Hall, R. O.: Sediment, water column, and open-channel denitrification in rivers measured using membrane-inlet mass spectrometry, Journal of Geophysical Research: Biogeosciences, 121, 1258-1274, 10.1002/2015jg003261, 2016.

Reisinger, A. J., Tank, J. L., Rosi-Marshall, E. J., Hall, R. O., and Baker, M. A.: The varying role of water column nutrient uptake along river continua in contrasting landscapes, Biogeochemistry, 125, 115-131, 10.1007/s10533-015-0118-z, 2015.

Reisinger, A. J., Tank, J. L., Hall, R. O., Rosi, E. J., Baker, M. A., and Genzoli, L.: Water column contributions to the metabolism and nutrient dynamics of mid-sized rivers, Biogeochemistry, 153, 67-84, 10.1007/s10533-021-00768-w, 2021.

https://doi.org/10.5194/egusphere-2023-3038
Preprint. Discussion started: 15 January 2024

Reynolds, C. S. and Descy, J.-P.: The production, biomass and structure of phytoplankton in large rivers, Large Rivers, 10, 161-187, 10.1127/lr/10/1996/161, 1996.

Rocher-Ros, G., Sponseller, R. A., Lidberg, W., Mörth, C. M., and Giesler, R.: Landscape process domains drive patterns of CO2 evasion from river networks, Limnology and Oceanography Letters, 4, 87-95, 10.1002/lol2.10108, 2019.

Rodríguez-Castillo, T., Estévez, E., González-Ferreras, A. M., and Barquín, J.: Estimating Ecosystem Metabolism to Entire River Networks, Ecosystems, 22, 892-911, 10.1007/s10021-018-0311-8, 2019.

Roley, S. S., Hall Jr., R. O., Perkins, W., Garayburu-Caruso, V. A., and Stegen, J. C.: Coupled primary production and respiration in a large river contrasts with smaller rivers and streams, Limnology and Oceanography, n/a, 15, https://doi.org/10.1002/lno.12435, 2023.

Running, S. and Zhao, M.: MOD17A3HGF MODIS/Terra Net Primary Production Gap-Filled Yearly L4 Global 500 m SIN Grid V006 [dataset], https://doi.org/10.5067/MODIS/MOD17A3HGF.006, 2019.

Running, S., Mu, Q., and Zhao, M.: MOD16A2 MODIS/Terra Net Evapotranspiration 8-Day L4 Global 500m SIN Grid V006 [dataset], https://doi.org/10.5067/MODIS/MOD16A2.006, 2017.

Savoy, P. and Harvey, J. W.: Predicting Light Regime Controls on Primary Productivity Across CONUS River Networks, Geophysical Research Letters, 48, 10.1029/2020gl092149, 2021.

Savoy, P., Bernhardt, E., Kirk, L., Cohen, M. J., and Heffernan, J. B.: A seasonally dynamic model of light at the stream surface, Freshwater Science, 40, 286-301, 10.1086/714270, 2021.

Savoy, P., Appling, A. P., Heffernan, J. B., Stets, E. G., Read, J. S., Harvey, J. W., and Bernhardt, E. S.: Metabolic rhythms in flowing waters: An approach for classifying river productivity regimes, Limnology and Oceanography, 64, 1835-1851, 10.1002/lno.11154, 2019.

Schiller, D., Datry, T., Corti, R., Foulquier, A., Tockner, K., Marcé, R., García-Baquero, G., Odriozola, I., Obrador, B., Elosegi, A., Mendoza-Lera, C., Gessner, M. O., Stubbington, R., Albariño, R., Allen, D. C., Altermatt, F., Arce, M. I., Arnon, S., Banas, D., Banegas-Medina, A., Beller, E., Blanchette, M. L., Blanco-Libreros, J. F., Blessing, J., Boëchat, I. G., Boersma, K. S., Bogan, M. T., Bonada, N., Bond, N. R., Brintrup, K., Bruder, A., Burrows, R. M., Cancellario, T., Carlson, S. M., Cauvy-Fraunié, S., Cid, N., Danger, M., Freitas Terra, B., Dehedin, A., De Girolamo, A. M., Campo, R., Díaz-Villanueva, V., Duerdoth, C. P., Dyer, F., Faye, E., Febria, C., Figueroa, R., Four, B., Gafny, S., Gómez, R., Gómez-Gener, L., Graça, M. A. S., Guareschi, S., Gücker, B., Hoppeler, F., Hwan, J. L., Kubheka, S., Laini, A., Langhans, S. D., Leigh, C., Little, C. J., Lorenz, S., Marshall, J., Martín, E. J., McIntosh, A., Meyer, E. I., Miliša, M., Mlambo, M. C., Moleón, M., Morais, M., Negus, P., Niyogi, D., Papatheodoulou, A., Pardo, I., Pařil, P., Pešić, V., Piscart, C., Polášek, M., Rodríguez-Lozano, P., Rolls, R. J., Sánchez-Montoya, M. M., Savić, A., Shumilova, O., Steward, A., Taleb, A., Uzan, A., Vander Vorste, R., Waltham, N., Woelfle-Erskine, C., Zak, D., Zarfl, C., and Zoppini, A.: Sediment Respiration Pulses in Intermittent Rivers and Ephemeral Streams, Global Biogeochemical Cycles, 33, 1251-1263, 10.1029/2019gb006276, 2019.

Segatto, P. L., Battin, T. J., and Bertuzzo, E.: The Metabolic Regimes at the Scale of an Entire Stream Network Unveiled Through Sensor Data and Machine Learning, Ecosystems, 10.1007/s10021-021-00618-8, 2021.

Shcherbakov, M. V., Brebels, A., Shcherbakova, N. L., Tyukov, A. P., Janovsky, T. A., and Kamaev, V. A. e.: A Survey of Forecast Error Measures, World Applied Sciences Journal, 24, 171-176, 10.5829/idosi.wasj.2013.24.itmies.80032, 2013.

Son, K., Fang, Y., Gomez-Velez, J. D., and Chen, X.: Spatial Microbial Respiration Variations in the Hyporheic Zones Within the Columbia River Basin, Journal of Geophysical Research: Biogeosciences, 127, 10.1029/2021jg006654, 2022.

Tank, J. L., Rosi-Marshall, E. J., Baker, M. A., and Hall, R. O., Jr.: Are rivers just big streams? A pulse method to quantify nitrogen demand in a large river, Ecology, 89, 2935-2945, 10.1890/07-1315.1, 2008.

https://doi.org/10.5194/egusphere-2023-3038
Preprint. Discussion started: 15 January 2024

Tank, S. E., Fellman, J. B., Hood, E., and Kritzberg, E. S.: Beyond respiration: Controls on lateral carbon fluxes across the terrestrial-aquatic interface, Limnology and Oceanography Letters, 3, 76-88, 10.1002/lol2.10065, 2018.

Tolić, N., Liu, Y., Liyu, A., Shen, Y., Tfaily, M. M., Kujawinski, E. B., Longnecker, K., Kuo, L.-J., Robinson, E. W., Paša-Tolić, L., and Hess, N. J.: Formularity: Software for Automated Formula Assignment of Natural and Other Organic Matter from Ultrahigh-Resolution Mass Spectra, Analytical Chemistry, 89, 12659-12665, 10.1021/acs.analchem.7b03318, 2017.

Trentman, M. T., Tank, J. L., Davis, R. T., Hanrahan, B. R., Mahl, U. H., and Roley, S. S.: Watershed-scale Land Use Change Increases Ecosystem Metabolism in an Agricultural Stream, Ecosystems, 10.1007/s10021-021-00664-2, 2021.

U.S. Geological Survey: C6 Aqua 250-m eMODIS Remote Sensing Phenology Metrics across the conterminous U.S. [dataset], https://doi.org/10.5066/F7PC30G1, 2019a.

U.S. Geological Survey: National Hydrography Dataset Plus Version 2 [dataset], 2019b.

Uzarski, D. G., Stricker, C. A., Burton, T. M., King, D. K., and Steinman, A. D.: The importance of hyporheic sediment respiration in several mid-order Michigan rivers: comparison between methods in estimates of lotic metabolism, Hydrobiologia, 518, 47-57, 10.1023/b:hydr.0000025056.18736.d6, 2004.

Vannote, R. L., Minshall, G. W., Cummins, K. W., Sedell, J. R., and Cushing, C. E.: The River Continuum Concept, Canadian Journal of Fisheries and Aquatic Sciences, 37, 130-137, 10.1139/f80-017, 1980.

Ward, N. D., Sawakuchi, H. O., Richey, J. E., Keil, R. G., and Bianchi, T. S.: Enhanced Aquatic Respiration Associated With Mixing of Clearwater Tributary and Turbid Amazon River Waters, Frontiers in Earth Science, 7, 10.3389/feart.2019.00101, 2019.

Ward, N. D., Sawakuchi, H. O., Neu, V., Less, D. F. S., Valerio, A. M., Cunha, A. C., Kampel, M., Bianchi, T. S., Krusche, A. V., Richey, J. E., and Keil, R. G.: Velocity-amplified microbial respiration rates in the lower Amazon River, Limnology and Oceanography Letters, 3, 265-274, 10.1002/lol2.10062, 2018.

Wieczorek, M. E., Jackson, S. E., and Schwarz, G. E.: Select Attributes for NHDPlus Version 2.1 Reach Catchments and Modified Network Routed Upstream Watersheds for the Conterminous United States (ver. 3.0, January 2021), https://doi.org/10.5066/F7765D7V, 2018.

Wise, D. R., Zuroske, M. L., Carpenter, K. D., and Kiesling, R. L.: Assessment of eutrophication in the Lower Yakima River Basin, Washington, 2004–07, U.S. Geological Survey, Reston, VA, 108, 2009.

Zarnetske, J. P., Haggerty, R., Wondzell, S. M., and Baker, M. A.: Dynamics of nitrate production and removal as a function of residence time in the hyporheic zone, Journal of Geophysical Research, 116, 10.1029/2010jg001356, 2011.

Zhang, M. and Chadwick, M. A.: Influences of Elevated Nutrients and Water Temperature from Wastewater Effluent on River Ecosystem Metabolism, Environmental Processes, 9, 10.1007/s40710-022-00597-5, 2022.